RICE UNIVERSITY

A PI3-Kinase Mediated Negative Feedback Regulates
Neuronal Excitability at the Drosophila Neuromuscular Junction

by

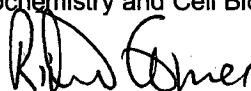**Eric Lane Howlett**

A THESIS SUBMITTED
IN PARTIAL FULFILLMENT OF THE
REQUIREMENTS FOR THE DEGREE
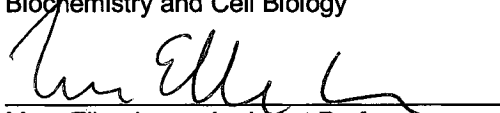
DOCTOR OF PHILOSOPHY
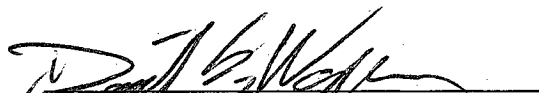
APPROVED, THESIS COMMITTEE:

Michael Stern, Professor
Biochemistry and Cell Biology

Richard Gomer, Professor
Biochemistry and Cell Biology

Mary Ellen Lane, Assistant Professor
Biochemistry and Cell Biology

Daniel Wagner, Assistant Professor
Biochemistry and Cell Biology

Michael Kohn, Assistant Professor
Ecology and Evolutionary Biology

HOUSTON, TEXAS
MAY 2009

UMI Number: 3362243

INFORMATION TO USERS

The quality of this reproduction is dependent upon the quality of the copy
submitted. Broken or indistinct print, colored or poor quality illustrations
and photographs, print bleed-through, substandard margins, and improper
alignment can adversely affect reproduction.
In the unlikely event that the author did not send a complete manuscript
and there are missing pages, these will be noted. Also, if unauthorized
copyright material had to be removed, a note will indicate the deletion.

UMI®

ABSTRACT

Use-dependent downregulation of neuronal activity (negative feedback) can act as a homeostatic mechanism to maintain neuronal activity at a particular specified value. Disruption of this negative feedback might lead to neurological pathologies such as epilepsy, but the precise mechanisms by which this feedback can occur remain incompletely understood. At one glutamatergic synapse, the Drosophila neuromuscular junction, a mutation in the group II metabotropic glutamate receptor gene (*DmGluRA*) increased motor neuron excitability by disrupting an autocrine, glutamate-mediated negative feedback. I show that *DmGluRA* mutations increase neuronal excitability by preventing PI3 kinase (PI3K) activation and consequently hyperactivating the transcription factor Foxo. Furthermore, glutamate application increases levels of phospho-Akt, a product of PI3K signaling, within motor nerve terminals in a *DmGluRA*-dependent manner. Finally, I show that PI3K increases both axon diameter and synapse number via the Tor/S6 kinase pathway, but not Foxo. In humans, PI3K and group II mGluRs are implicated in epilepsy, neurofibromatosis, autism, schizophrenia and other neurological disorders; however, neither the link between group II mGluRs and PI3K, nor the role of PI3K-dependent regulation of Foxo in the control of neuronal excitability, had been previously reported. My work suggests that some of the deficits in these neurological disorders might result from disruption of glutamate-mediated homeostasis of neuronal excitability.

ii

Acknowledgments

I would particularly like to thank my thesis adviser, Dr. Michael Stern, for all of his support over the years. His patience, guidance, and wisdom has molded me into the researcher I am today, and has set a remarkable example of the scientist I would like to become. In addition, I would like to thank my thesis committee: Drs. Mary Ellen Lane, Richard Gomer, and Daniel Wagner for their guidance and invaluable experimental suggestions throughout my graduate career.

I would also like to thank current and former members of the Stern lab for their assistance, advice, and support, both in science and in life: Magdalena Walkiewicz, Chun-Jen "Curtis" Lin, Dr. Robert Cardnell, Dr. Veronica Hall, William Lavery, Shelly Wells, Ming Yang, Elaina Bolinger, Alexandra Mirina, Yara Hamade, Alec Marin, Erica Han, and Jason Mishaw. I will miss you guys.

I wouldn't have made it through the last six years if it hadn't been for my wonderful friends who have been there through thick and thin. In particular I'd like to thank Chris Holterhoff, Joseph Faust, Cassidy Johnson, and Sol Gomez de la Torre Canny. Most notably, I'd like to thank Bethany Morehouse, my best friend and the love of my life, for her undying wellspring of love and support.

Finally, I would like to thank my family for all of their support over the years and for raising me to be the person I am today. You have always believed in me and have done everything possible to help me reach my goals, and for that I am eternally grateful.

iii

Table of Contents

Chapter 1: Background

Chapter 2: Methods

Chapter 3: Results

Chapter 4: Discussion

Chapter 5: The effects of larval nutrition on neuronal excitability

and   nmj   growth

Chapter 6: Referenced Works...81

Chapter 7: Appendices 96

List of Figures and Tables

viii

List of Relevant Gene Names

AKH   *adipokinetic hormone*

Akt   *akt*

CaM   *calmodulin*

CFP   *cyan fluorescent protein*

D42   *motor neuron specific Gal4 driver*

dilp2   *drosophila insulin like peptide 2*

eag   *ether-a-go-go (K+ channel subunit)*

FAK   *focal adhesion kinase*

FoxO   *forkhead transcription factor*

frq   *frequenin, Drosophila NCS-1 homolog*

GFP   *green fluorescent protein*

gli   *gliotactin*

Glued   *p150-Glued subunit of the dynactin complex*

GSK3   *glycogen synthase kinase 3*

Hk   *hyperkinetic (K-channel subunit)*

Homer   *metabotropic glutamate receptor binding protein*

HRP   *horseradish peroxidase*

IGF   *insulin-like growth factor*

IP3R   *inositol 1,4,5-triphosphate receptor*

x

AKH   adipokinetic hormone

IRS   insulin receptor substrate

NCS-1 neuronal calcium sensor 1

NF1   neurofibromin 1

OK6   motor neuron specific Gal4 driver

p110   PI3K catalytic subunit

p85   PI3K regulatory subunit

para   paralytic

PDK1   pyruvate dehydrogenase kinase, isozyme 1

PDK2   pyruvate dehydrogenase kinase, isozyme 2

PI3K   phosphoinositide 3-kinase

PICK-1 protein interacting with C kinase 1

PTEN   phosphatase and tensin homolog on chromosome 10

pum   pumilio

Ras   Ras GTPase

Rheb   Ras homolog enriched in brain

rpr   reaper

S6K   S6 kinase

sh   shaker (K channel subunit)

tor   target of rapamycin

YFP   yellow fluorescent protein

xi

AKH   *adipokinetic hormone*

List of Abbreviations

Act   constitutively active

AMPA   a-amino-3-hydroxy-5-methyl-4-isoaxolepropionic aci

Ca^{2+} calcium ion

CAAX   C-terminal post-translational modification site allowing for membrane

            targeting

CC   corpus cardiacum

Cl^- chloride ion

CNS   central nervous system

DmGluRA Drosophila metabotropic glutamate receptor

DN   dominant negative

E_i electrochemical potentials of relevant ion species

E_m electrochemical membrane potenial

ejp   excitatory junction potential

FRET   Forster resonance energy transfer

GAL4   transcription factor

GECI   genetically enncoded calcium indicator

GPCR   G-protein coupled receptor

IPC   Insulin producing cell

K^+ potassium ion

LTD   long term depression

xiii

Act	constitutively active
LTF	long term facilitation
LTP	long term potentiation
mGluR	metabotropic glutamate receptor
Na^+	sodium ion
NMDA	N-methyl-D-aspartate
nmj	neuromuscular junction
PBS	phosphate buffered saline
PH	pleckstrin homology domain
PIP_2	Phosphatidylinositol 4,5-bisphosphate
PIP_3	Phosphatidylinositol 3,4,5-triphosphate
PNS	peripheral nervous system
PtdIns	phosphatiylinositol
RNAi	RNA interference
s880	Stern lab Wildtype stock
SH2	Src Homology 2
SH3	Src Homology 3
UAS	upstream activating sequence

Chapter 1: Background

1.1   Significance

Negative Feedback Processes

Negative feedback processes, which can enable maintenance of neuronal homeostasis, are widely observed in neuronal systems (Marder and Prinz, 2003; Davis, 2006; Pozzi et al., 2008). For example, neuronal silencing via tetrodotoxin application both *in vivo* and *in vitro* increases excitability (Desai et al., 1999; Gibson et al., 2006; Echegoyen et al., 2007). This effect occurs *in vitro* via both increased sodium currents and decreased potassium currents. However, the signaling pathways responsible for these excitability changes remain unclear. In addition, a number of neurological disorders are associated with changes in excitability due to alterations of neuronal homeostasis: epilepsy, autism, anxiety disorders, and others. Consequently, increasing my understanding of the mechanisms responsible for maintaining proper neuronal homeostasis is of substantial importance.

1

1.2   Drosophila peripheral nerves

Drosophila peripheral nerves consist of bundles of motor and sensory axons that are each individually ensheathed in a layer of wrapping glia which are analogous to Schwann cells in mammals (Sepp et al., 2000; Stork et al., 2008). This bundle of ensheathed axons and wrapping glia is then itself ensheated in an outer layer of subperineurial glia followed by a second outer layer of perineurial glia, which is hypothesized to provide structural support to the peripheral nerve (Yager et al., 2001; Stork et al., 2008).

1.3   Action potential propagation and Synaptic Transmission

The axonal membrane potential is derived from the relative balance of charged ion species on either side of the membrane. This potential can be described mathematically by the Goldman Constant Field Equation in which the resting electrochemical potential of the membrane (E_m) is the sum of the individual electrochemical potentials of each of the relevant ion species (E_i).

$$E_m = -\frac{RT}{F}\ln\left(\frac{P_K[K]_o + P_{Na}[Na]_o - P_{Cl}[Cl]_o}{P_K[K]_i + P_{Na}[Na]_i - P_{Cl}[Cl]_i}\right)$$ *"Goldman Constant Field Equation"*

The electrochemical potentials for the individual ion species can be derived using the Nernst Equation.

2

$$E_i = (E_2 - E_1) = -\frac{RT}{zF}\left(\frac{C_2}{C_1}\right)$$ *"Nernst Equation"*

Because Cl⁻ ions are isotonic on both sides of the membrane, E_m can be further

simplified into the Mullins and Noda steady state equation in which r is the

coupling ratio of the Na⁺/K⁺ pump that maintains the electrochemical gradient,

and b is the ratio of membrane permeability to Na⁺ and K⁺ respectively.

$$E_m = 58\log\left(\frac{r[K]_o + b[Na]_o}{r[K]_i + b[Na]_i}\right)$$ *"Mullins-Noda Steady State Equation"*

Axonal membranes at rest are maintained at a negative resting potential.

Stimulation of the neuron at the axon hillock can generate a small depolarization

of the membrane (see figure 1.1). If the depolarization is beyond the stimulation

threshold, voltage-gated sodium channels will open, increasing the membrane's

permeability to Na⁺ ions in a localized region, thus leading to an increase in 'b'.

Diffusing down their electrochemical gradient, Na⁺ ions then flow into the neuron

resulting in further depolarization of the membrane potential. As this

depolarization spreads outwards from its source, a positive feedback is

generated triggering the opening of other voltgage-gated sodium channels, thus

creating a wave of depolarization traveling down the axon. In addition to

triggering the opening of sodium channels, the depolarization triggers the

opening of voltage-gated potassium channels, subsequently increasing the

membrane's permeability to K⁺ ions. In the initial phases of the action potential,

the Na⁺ influx is greater than the K⁺ efflux, thus creating a rise in the membrane

3
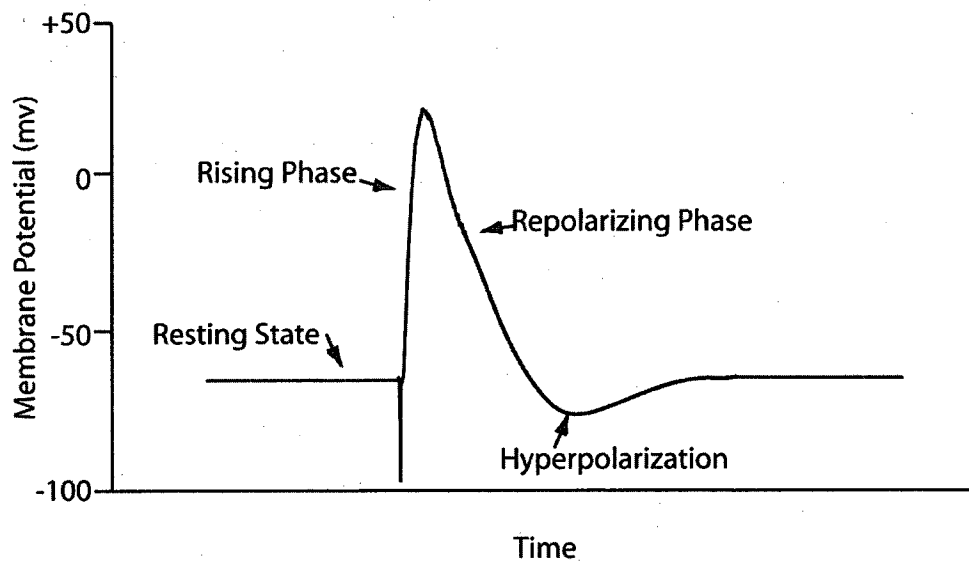
Figure 1.1. Schematic of action potential propagation. When a neuronal membrane is disturbed from the resting state by a stimulus, and the subsequent depolarization is sufficient to cause the opening of voltage gated Na^+ channels, and action potential will be generated. The subsequent influx of Na^+ ions causes further depolarization leading to the rising phase of the action potential. After the initial opening, Na^+ channels will close and remain inactive, thus allowing a directional propagation of signal. As the action potential reaches the peak of depolarization, votage-gated K^+ channels open, allowing for an efflux of K^+ ions initiating the repolarizing phase. There is a brief overshoot of polarization, leading to the hyperpolarized state, after which the membrane returns to its resting state.

4

potential. As the Na^+ channels reach a maximal opening and the membrane potential reaches its peak, Na^+ channel inactivation allows the K^+ efflux to repolarize the cell. This repolarization overshoots the resting potential causing a hyperpolarization, after which the neuron is in a brief refractory period due to Na^+ channel inactivation during which further action potential propogation cannot occur. As the action potential reaches the nerve terminal, the depolarization induces the opening of voltage-gated calcium channels, allowing the influx of Ca^{2+} ions from the extracellular environment. This Ca^{2+} influx then triggers the Snare-mediated release of vesicles containing neurotransmitter into the synapse and the subsequent diffusion of the neurotransmitter across the synaptic cleft to the postsynaptic cell.

Because action potential propagation is dependent on the alteration of membrane permeability by ion channels, it stands to reason that neuronal excitability, or the propensity of a neuron to fire an action potential, is directly related to the ratio of different species of ion channels present in the membrane.

1.4   Long term facilitation (LTF) as a measure of neuronal excitability

Alterations in neuronal excitability are manifested by an increased rate of onset of a form of synaptic plasticity termed long-term facilitation (LTF) (Jan and Jan, 1978; Bogdanik et al., 2004), which is induced when a motor neuron is subjected to repetitive nerve stimulation at low bath $[Ca^{2+}]$. At a certain point in

5

the stimulus train, an abrupt increase in transmitter release and hence muscle depolarization (termed excitatory junctional potential, or ejp) is observed (Figure 3.2 A). LTF not only increases ejp amplitude, but also ejp duration, indicative of prolonged and asynchronous transmitter release (Figure 3.2 A). This abrupt increase in the amount and duration of transmitter release is caused by an abrupt increase in the duration of nerve terminal depolarization and hence Ca^{2+} influx, and reflects a progressive increase in motor neuron excitability induced by the repetitive nerve stimulation: when an excitability threshold is reached, LTF occurs (Jan and Jan, 1978; Stern and Ganetzky, 1989; Stern et al., 1990).

In Drosophila, many genotypes that increase motor neuron excitability by decreasing K^+ currents or increasing Na^+ currents increase the rate of onset of LTF. For example, altered activities of *frequenin* and *Hyperkinetic*, which act via K^+ channels, or *paralytic* and *pumilio*, which act via Na^+ channels, each increase the rate of onset of LTF (Loughney et al., 1989; Stern and Ganetzky, 1989; Stern et al., 1990; Mallart et al., 1991; Chouinard et al., 1995; Schweers et al., 2002; Mee et al., 2004). By increasing motor neuron excitability, the genotypes described above apparently bring excitability closer to the threshold required to evoke LTF and consequently decrease the number of prior nerve stimulations required to reach this threshold. In these genotypes, the prolonged nerve terminal depolarizations that triggered LTF were revealed by recording ejps and simultaneously recording extracellularly electrical activity within the peripheral nerves during LTF onset. It was found that LTF onset was accompanied by the appearance within peripheral nerves of supernumerary action potentials

6

occurring at about 10 msec intervals following the initial induced action potential (Ganetzky and Wu, 1982; Loughney et al., 1989; Stern and Ganetzky, 1989; Stern et al., 1990; Mallart et al., 1991; Chouinard et al., 1995; Schweers et al., 2002; Mee et al., 2004). Several lines of evidence suggested that these supernumerary action potentials arose in motor axons and were responsible for the increased transmitter release underlying LTF. First, the number of these supernumerary action potentials correlated with ejp duration, and second, these supernumerary action potentials often preceded depolarizing steps in the asynchronous, multi-step ejps that occurred after LTF onset. Similar supernumerary action potentials were observed following nerve stimulation in the *eag Sh* double mutant, in which two distinct K channel α subunits are simultaneously eliminated, and which consequently exhibits extreme neuronal hyperexcitability. In the *eag Sh* double mutant, these supernumerary action potentials arise in the motor nerve terminals and exhibit retrograde propagation (Ganetzky and Wu, 1982). It was suggested that the supernumerary action potentials were caused by, and also prolonged, motor nerve terminal depolarization, and thus participated in a positive feedback loop prolonging depolarization (Ganetzky and Wu, 1982). This positive feedback loop presumably underlies the abrupt, threshold-like onset of LTF.

1.5   Metabotropic glutamate receptors (mGluRs)

7

The amino acid glutamate is a critical signaling molecule in the nervous system, acting as the principle excitatory neurotransmitter in the mammalian CNS (Watkins and Evans, 1981) and the arthropod nmj, and can act on two classes of receptors. One class, ionotropic glutamate receptors, comprises ligand gated mutlimeric ion-channels and can be divided into three distinct types based on their associated agonists: NMDA (N-methyl-D-aspartate), AMPA (α-amino-3-hydroxy-5-methyl-4-isoaxolepropionic acid), and kainate receptors. As ion channels, these receptors allow glutamate to act in fast excitatory neurotransmission, often postsynaptically at glutamatergic synapses. The second class of glutamate receptors, metabotropic glutamate receptors (mGluRs) are coupled to heterotrimeric G-proteins which allow them to link glutamate signaling to intracellular second messenger systems. As such, mGluRs provide slow modulation of assorted functions (reviewed in Ferraguti and Shigemoto, 2006) including excitatory (Glaum and Miller, 1992) and inhibitory (Fiorillo and Williams, 1998) transmission, long term potentiation (Bortolotto and Collingridge, 1993) and long term depression (Linden and Connor, 1992), and are also involved in numerous processes such as neuronal development (Catania et al., 2001), and learning and memory (Aiba et al., 1994). In addition mGluRs have been implicated in neurological disorders such as epilepsy, schizophrenia, Parkinson's, anxiety, Fragile X mental retardation, and others (Enz, 2007). Collectively, these features make mGluRs an attractive subject of research to gain a better understanding of neuronal homeostasis.

8

1.5.1 Function and Structure of mGluRs

The first evidence of metabotropic glutamate receptors came from experiments showing that glutamate, when applied to cultured striatal neurons, stimulated enhanced hydrolysis of phosphoinositides (Sladeczek et al., 1985). By demonstrating that glutamate could stimulate metabolic processes beyond the fast excitatory transmission exhibited by ionotropic receptors, this observation suggested that there was a second type of glutamate receptor acting in these systems. Similar experiments in other brain preparations confirmed these results: cultured cerebellar granule cells, rat brain slices, rat brain synaptoneurosomes, and cultured glial cells (reviewed in Schoepp et al., 1999; Sepp et al., 2000) Further experimentation performed in *Xenopus* oocytes injected with rat brain mRNA showed that application of glutamate and its analogue quisqualate, but not NMDA or kainate, were able to initiate inositol phospholipid metabolism, formation of IP3, and subsequent mobilization of Ca^{2+} from internal stores (Sugiyama et al., 1987). In addition, Joro Spider toxin, an inhibitor of ionotropic glutamate receptors, was unable to block the mobilization of Ca^{2+} by quisqualate. Taken together, these data confirmed the existence of mGluRs as a receptor class independent of the known ionotropic receptors. Lastly, Sugiyama et al. (1987) showed that glutamate induced Ca^{2+} mobilization

9
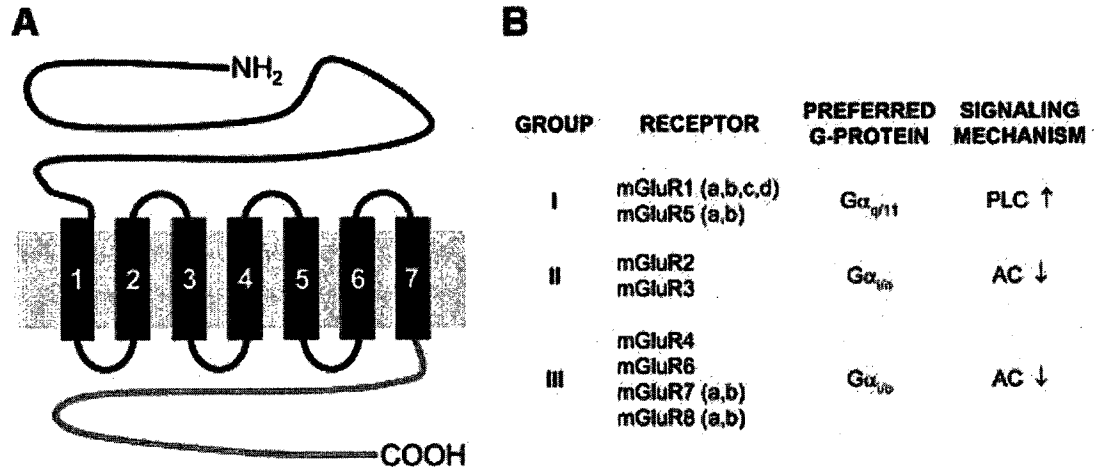
Figure 1.2 Topological schematic and classification of mGluRs. A) mGluRs consist of 7 transmembrane domains. All groups of mGluRs have a high degree of conservation in the transmembrane domains and N terminal. The intracellular C-terminal, however, varies widely between different mGluR receptor types. B) mGluRs are divided into three groups based on sequence homology, preferred G-protein, pharmacological properties, and consequential signaling mechanisms. Group I mGluRs most often associate are often excitatory, whereas Group II and Group III mGluRs are usually inhibitory. Image take from (Enz, 2007).

10

was inhibited by the addition of pertussis toxin, suggesting that mGluR activity was mediated by G_o or G_i. Rat mGluR1a, the first mGluR cloned, was expression-cloned using a rat cerebellar library (Houamed et al., 1991; Masu et al., 1991). In short succession, seven other mGluR types were identified based on their sequence homology to mGluR1a, named mGluR2-8 in order of their discovery. These receptors fall into three distinct groups, differentiated by sequence homology, associated signal- transduction mechanisms, and pharmacological properties (Enz, 2007) (Figure 1.2).

Like all G-protein coupled receptors (GPCRs), mGluR's consist of seven hydrophobic transmembrane domains linked by three intracellular loops and four extracellular loops (for review see Schoepp, 2001 and the references within). The N-terminal consists of a highly conserved extracellular ligand-binding domain of about 600 amino acids which recognizes glutamate and its analogues (O'Hara et al., 1993). The intracellular C-terminus, which physically interacts with the associated G-proteins, can vary between 37 and 377 amino acids in length depending on the receptor type, and it is this diversity which is responsible for the variety of functions carried out by the individual receptor types. This differs from other GPCRs in which the specificity and activation of the associated G proteins is carried out by the third intracellular loop (Pin et al., 1994).

1.5.2 Mammalian roles in neuronal homeostasis

11

The mammalian group II metabotropic glutamate receptors, are well positioned to mediate negative feedback. When localized presynaptically, these receptors can act as autoinhibitors of glutamate release (Scanziani et al., 1997; Kew et al., 2001; Chen et al., 2002; Poisik et al., 2005). Because these receptors are located outside of the active zone (Schoepp, 2001), activation is thought to occur only during conditions of elevated glutamate release and might serve to prevent glutamate-mediated neurotoxicity. Agonists for these receptors are proposed for treatment of schizophrenia, anxiety and epilepsy, among others (Swanson et al., 2005; Patil et al., 2007), but the mGluR-dependent signaling pathways that underlie these disorders remain unidentified. Furthermore, although many of the acute effects of group II mGluR activation on neuronal physiology have been elucidated (Anwyl, 1999; Alexander and Godwin, 2006), possible long term effects on neuronal function, such as through changes in ion channel gene expression, remain essentially unexplored.

1.5.3 Drosophila mGluRA (DmGluRA)

In Drosophila, the single *DmGluRA* gene encodes a protein most similar to the mammalian group II mGluR (Bogdanik et al., 2004). DmGluRA is located presynaptically at the neuromuscular junction (nmj), which suggests that DmGluRA might regulate transmitter release from motor neurons. Elimination of *DmGluRA* by the null mutation *DmGluRA[112b]*, or by RNAi-mediated *DmGluRA* knockdown specifically in motor neurons, increases neuronal excitability

12

(Bogdanik et al., 2004). Given that glutamate is the excitatory neurotransmitter from Drosophila motor neurons, the increased excitability of *DmGluRA* mutants raised the possibility that DmGluRA decreases motor neuron excitability upon activation by glutamate released from motor nerve terminals. In this view, DmGluRA would mediate an activity-dependent negative feedback on excitability. However, the mechanism by which this negative feedback is accomplished was not elucidated.

1.6   PI3K/AKT signaling

Phosphatidylinositol 3-kinases (PI3K)s represent a family of enzymes capable of phosphorylating the 3'-hydroxyl group on the inositol ring of phosphatidylinositol (PtdIns), PtdIns 4-phosphate, or PtdIns 4,5-bisphosphate (Panayotou, 1998). This activity is responsible for a host of signal transduction cascades within the cell including but not limited to: DNA synthesis, cell survival, membrane ruffling, chemotaxis, cytoskeletal rearrangements, oocyte maturation, glucose transport, and vesicle trafficking (Panayotou, 1998). PI3K is comprised of two subunits, a 1,068-aa catalytic subunit called p110, and a 724-aa regulatory subunit called p85. p85 has several functional domains within its structure, including two SH2 domains, an SH3 domain, and a BCR domain. These domains serve to interact with activated tyrosine-phosphorylated molecules

13
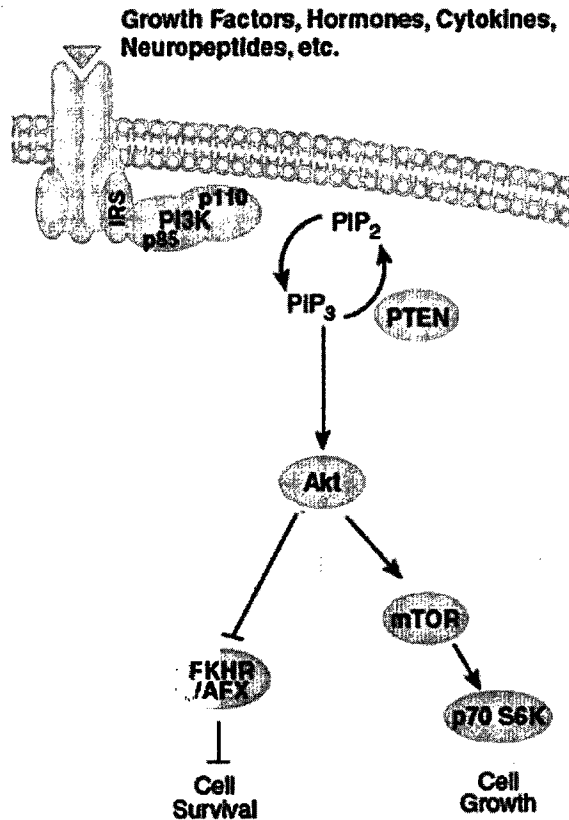
Figure 1.3. PI3K activity regulates many downstream effectors. PI3K is activated by receptor tyrosine kinases such as the insulin receptor shown here. PI3K phosphorylates the 3' hydroxyl group on the inositol ring of PIP_2 thus generating PIP_3. The presence of PIP_3 in the cell membrane recruits proteins containing pleckstrin homology (PH) domains, such Akt, to the membrane. Here, Akt is phosphorylated and activated, thus going on to phosphorylate a number of downstream targets including the forkhead transcription factor Foxo, and the Tor/S6K pathway. *Image adapted from Cell Signaling Technology.*

within the membrane (Panayotou, 1998). The p110 catalytic subunit is then

recruited to the membrane via its association with p85 and brought into proximity

14

with its phospoinositide substrates, setting the stage for their phosphorylation (Figure 1.3). In addition to activation by receptor tyrosine kinases, the small GTP-ase Ras via its direct interaction with the p110 catalytic subunit can activate PI3K. Phosphatase and tensin homolog on chromosome 10 (PTEN) is another molecule important to phosphoinositide signaling. As its name suggests, PTEN has phosphatase activity specific to the 3'hydroxyl group on the inositol ring of PtdIns. Together, PI3K and PTEN serve to tightly regulate phosphoinositide signaling at the membrane.

One of the downstream effectors of PI3K of interest to the Stern lab is the serine/threonine protein kinase Akt. Akt contains a pleckstrin homology domain (PH) to which PIP3 binds causing the subsequent translocation of Akt to the membrane (Hay and Sonenberg, 2004). Here, Akt is activated by the phosphorylation of residues 342 and 505 by PDK1 and PDK2, both of which are necessary for Akt activation (Figure 1.3). Akt subsequently acts in a signaling pathway that results in the regulation of cell growth and proliferation through mTOR signaling (Hay and Sonenberg, 2004).

1.7   Gal4/UAS system

The Gal4/ UAS system is a powerful genetic tool that allows for ectopic expression of genes of interest in a tissue and temporal specific manner within

15

an organism. It utilizes the yeast transcription factor Gal4 in order to drive expression of a gene placed under the control of the Gal4 upstream activating sequence (UAS) (Brand and Perrimon, 1993). The expression of *Gal4* is placed under the regulatory control of a gene with a desired expression pattern (Figure 1.4). In flies carrying the *Gal4* transgene, Gal4 will be present in whichever cell types the regulatory control gene is present. Being an transcription factor exclusively found in yeast, the presence of Gal4 by itself within Drosophila cells is unlikely to lead to the activation of Drosophila genes. However, a second fly line carrying a gene of interest under the regulatory control of the *UAS* sequence can then be crossed to the Gal4 line. Within the progeny of this cross, Gal4 will bind to the UAS in the tissues in which Gal4 is present. This thus allows one to drive expression of a desired gene under UAS control in whatever tissue the Gal4 driver expresses Gal4.
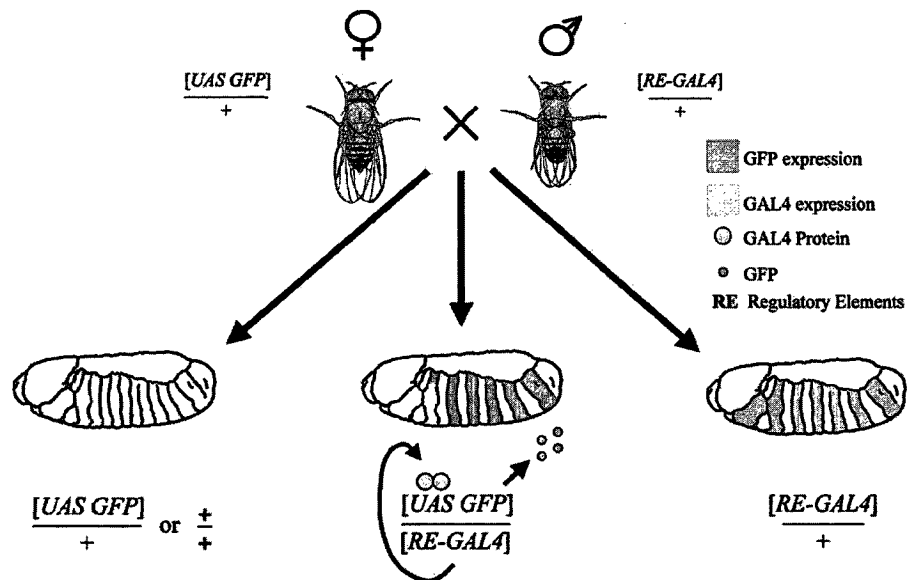
Figure 1.4 Schematic of the Gal4/UAS system. The Gal4/UAS system allows for the temporal and tissue specific expression of transgenes of interest. Fly lines expressing the yeast transcription factor Gal4 under the control of regulatory elements from a gene with a desired expression pattern are crossed to fly lines containing a gene of interest under the regulatory control of the upstream activating sequence (UAS). The progeny of these flies will express the UAS-regulated transgene in the expression pattern of the Gal4 transgene. *Image taken from (Duffy, 2002).*

17

Chapter 2: Methods and Materials

2.1 Maintenance of fly stocks and crosses

Fly stocks were maintained on standard cornmeal/ agar Drosophila media at room temperature. *D42* and *OK6* express *Gal4* in motor neurons and were provided by Tom Schwarz, Boston, Massachusetts, and Hermann Aberle, Tubingen, Germany respectively. The *UAS-PI3K^{DN}* (D954A) and *UAS-PI3K-CAAX* transgenes were provided by Sally Leevers, London, UK, the *UAS-Foxo^{+}* transgene was provided by Marc Tatar, Providence, RI, the *Foxo^{21}* and *Foxo^{25}* lines were provided by Heinrich Jasper, Rochester, NY, the *UAS-S6K^{DN}* and *UAS-S6K^{act}* transgenes were provided by Ping Shen, Athens, GA, and the *UAS-DmGluRA-RNAi* and the *DmGluRA^{112b}* lines were provided by Marie-Laure Parmentier, Montpelier, France. All other fly stocks were provided by the Drosophila stock center, Bloomington, IN.

The *D42* motor neuron driver was used to express transgenes for almost all experiments, except that the *OK6* driver was used for experiments where the *Foxo^{21}/Foxo^{25}* genotype was included. *OK6* is located on a different chromosome from *Foxo*, which simplifies stock construction.

Fly husbandry was preformed as previously described (Greenspan, 1997).

2.2 Larval micro-dissection

18

Wandering 3rd instar larvae were grown in uncrowded bottles at 23°C and collected from the bottle within 2 days of the first observation of the presence of wandering third instar larvae. Larva were pinned ventral side down to a dissection plate using magnetically retained insect pins and eviscerated in a standard saline solution for electrophysiology, or in PBS-T for Immunocytochemistry leaving only an intact central and peripheral nervous system and body wall muscles. Special care was taken not to damage or pull the nerves away from the nmj. The peripheral nerves were then severed immediately posterior to the ventral ganglia, leaving them attached only at the nmj (Figure 2.1). The resulting larval pelt contains seven repeating abdominal hemi-segments, each with repeating overlapping sets of abdominal muscles. For my work, only muscles 7 and 6 were used.

2.3 Immunocytochemistry

2.3.1 Bouton counts

FITC conjugated antibodies against horseradish peroxidase (HRP) were raised in goat (Jackson ImmunoResearch) and were used at 1:400 dilution. Antibodies against Drosophila p-Akt (Ser505) were raised in rabbit (Cell Signaling Technologies) and were used at 1:500 dilution. Rhodamine Red

19
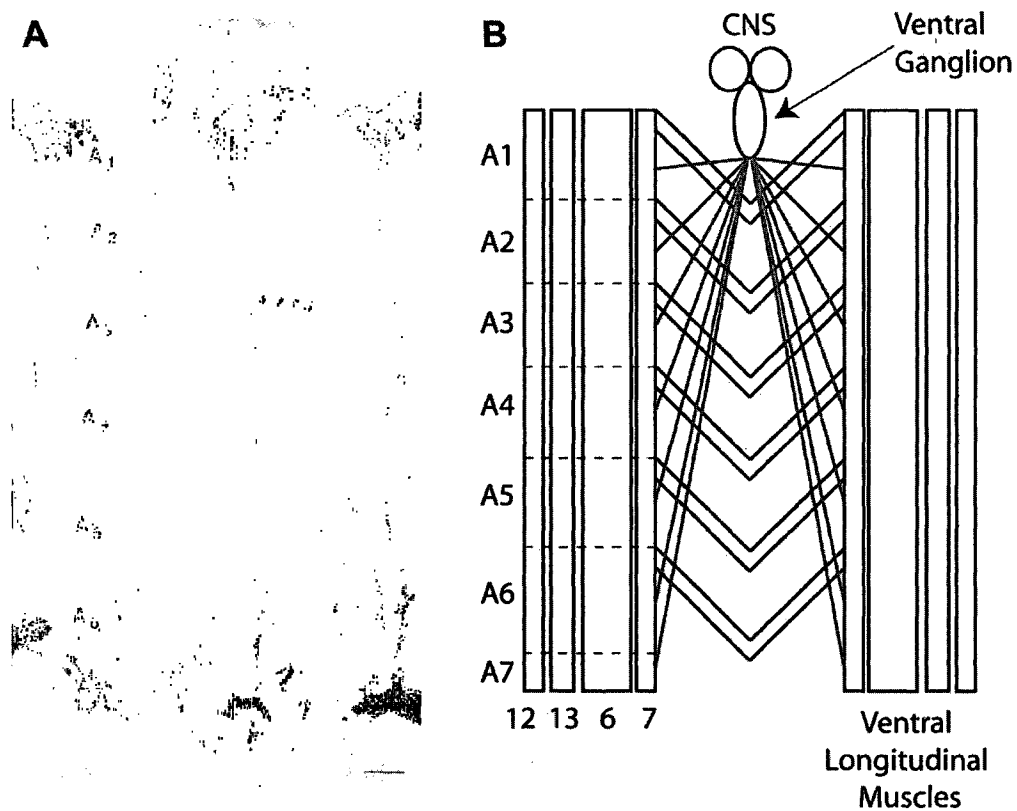
Figure 2.1 Wandering 3rd instar larval preparation. *A*, Toluidine-blue-stained preparation of *Drosophila* 3rd instar larvae (adapted from Budnik et al., 1990). *B*, Schematic drawing of larval preparation. The body wall muscles of are divided into 7 repeating abdominal hemi-segments each innervated by a peripheral nerve radiating from the ventral ganglion. Ventral longitudinal muscles 6 and 7 at segments A3 and A4 were used for arborization measurements, and muscle 6 was used for intracellular muscle recordings of ejps. Scale bar = 200 μm

20

conjugated goat anti-rabbit (Jackson ImmunoResearch) was used at a dilution of 1:1000. For arborization measurements, larvae were dissected in PBS-T and fixed in 4% paraformaldehyde. Images were taken on a Zeiss 410 laser scanning confocal microscope (LSM) with a 20x objective. ImageJ was used to obtain surface area measurements of muscle 6 from abdominal segment A3, and the number of boutons was counted manually.

2.3.2 P-Akt measurements

For p-Akt measurements, larvae were dissected in Grace's insect cell culture media (Gibco). When glutamate was applied,100 μM glutamic acid monosodium salt monohydrate (Acros Organics) dissolved in Grace's insect cell culture media was added to the well of the dissection plate. 1 minute after glutamate addition, larvae were rapidly washed in standard saline (0.128 M NaCl, 2.0 mM KCl, 4.0 mM $MgCl_2$, 0.34 M sucrose, 5.0 mM HEPES, pH 7.1, and 0.15 mM $CaCl_2$), and then immediately fixed in 4% paraformaldehyde. For the 10 min wash, the larvae were washed in Grace's insect cell culture media and placed on shaker for 10 minutes before fixing. Care was taken to treat all samples identically during this procedure. Images were taken on a Zeiss 510 LSM with a 20x objective. Z-stacks were compiled from 2 μm serial sections to a depth adequate to encompass the entire bouton thickness for each sample (from 8-20 μm). Muscles 7 and 6 from either abdominal segments A3 or A4 were used for measurements. ImageJ software was used to analyze p-Akt intensities. In particular, 2D projections were created using the median pixel intensity from

21

each stack at each coordinate point. Neuronal structures, marked by anti-HRP, were traced using the freehand selection tool and the selection was transferred to the anti-p-Akt image where the mean pixel intensity value was measured. Background was obtained with a selection box encompassing the non-neuronal area of muscles 6 and 7 in the particular abdominal segment, the mean pixel intensity was measured and subtracted from the mean p-Akt pixel intensity.

2.4 Electrophysiology

2.4.1 Ejp recordings

Larvae were grown to the wandering third-instar stage in uncrowded bottles at room temperature and dissected as described (Jan and Jan, 1978; Stern and Ganetzky, 1989) in standard saline solution (128 mM NaCl, 2.0 mM KCl, 4.0 mM MgCl$_2$, 34 mM sucrose, 5.0 mM HEPES, pH 7.1, and CaCl$_2$ as specified in the text). Peripheral nerves were cut posterior to the ventral ganglion and were stimulated using a suction electrode (Figure 2.2). Muscle recordings were taken from muscle 6 in abdominal sections 3-5. Stimulation intensity (5 V for approximately 0.05 msec) was adjusted to 1.5 times threshold, which reproducibly stimulates both axons innervating muscle cell 6. Recording electrodes were pulled using a Flaming/Brown micropipette puller to a tip resistance of 10-40 mΩ and filled with 3M KCl. ejp amplitude data are reported as geometric, rather than arithmetic means, because the data show a positive skew.

22

2.4.2 Long term facilitation (LTF)

Larvae were dissected and recordings performed as described in section 2.5.1, with the exception that, unless otherwise noted, the bath solution contained 0.15 mM $[Ca^{2+}]$ and 100 µM quinidine, which is a K^+ channel blocker that sensitizes the motor neuron and enables LTF to occur and be measured even in hypoexcitable neurons. The number of stimulations required to reach LTF was recorded at 4 stimulation frequencies, 3Hz, 5Hz, 7Hz, and 10Hz. LTF data are reported as geometric, rather than arithmetic means, because the data show a positive skew.

2.4.3 Extracellular nerve recordings

For extracellular recordings of neuronal action potentials, a loop of nerve near the nerve terminal was introduced into a suction electrode and nerve activity recorded with a DAM-80 differential amplifier.

2.4.4 Failures

The failure of an action potential to elicit a release of neurotransmitter, otherwise known as a failure, is a condition that is directly dependent on external $[Ca^{2+}]$. Larvae were dissected and recordings performed as described in section 2.5.1. The percentage of successful ejp's out of the total number of stimulations is plotted as a percentage. Failures were measured under 3 different external $[Ca^{2+}]$'s, 0.1mM, 0.15mM, and 0.2mM conditions.

23
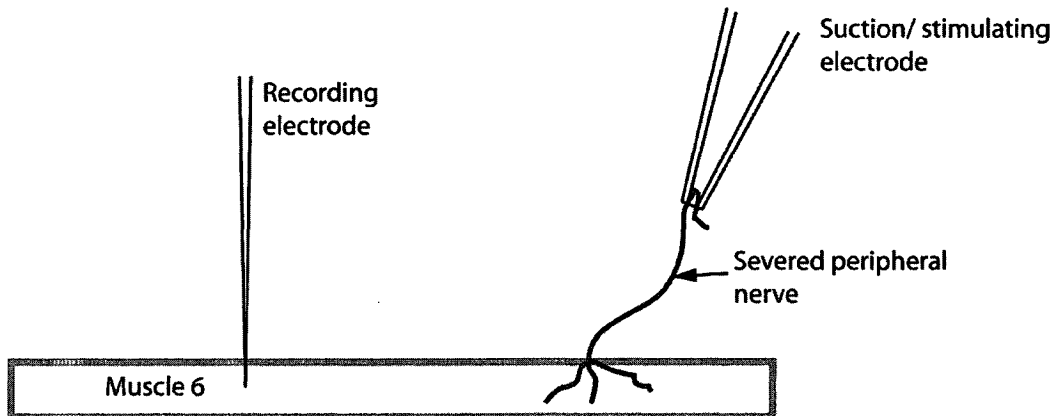
Figure 2.2   Larval nmj preparation. A loop of the severed peripheral nerve (purple) is sucked into a micro-bore glass suction/stimulating electrode. The nerve is then stimulated, generating an action potential and subsequent neurotransmitter release at the nmj. The muscle's (green) depolarization in response to this evoked neurotransmitter release is recorded using a second glass recording electrode.

24

2.5 Electron Microscopy

Larvae were grown to the wandering third-instar stage in uncrowded bottles at room temperature. Dissections and preparation for microscopy were performed as previously described (Yager et al., 2001). Nerve cross sections close to (within about 10 μm from) the ventral ganglion were obtained and analyzed. Axon diameter measurements were taken from the five largest axons from five different nerves from at least two different larvae.

2.6 Ca^{2+} measurements

The Cameleon 2.1 transgene is a powerful tool for analyzing changes in [Ca^{2+}] within a cell. The transgene encodes *calmodulin* (*CaM*) and the sequence for the calmodulin target peptide M13 flanked on either side by a yellow fluorescent protein (YFP) and cyan fluorescent protein (CFP) fluorophores. In the absence of Ca^{2+}, the Cameleon sensor is elongated, and the two fluorophores are excited by and emit light under their respective excitation/emission spectra. In the presence of Ca^{2+}, however, the CaM binds the Ca^{2+} and the Cameleon undergoes a conformational change, bringing the two fluorophores into close proximity thus allowing for Fö rster resonance energy transfer (FRET) to occur. Under these conditions, when excited in the 440 nm range appropriate for excitation of CFP, the CFP will transfer energy to the YFP, and light will be emitted at 535 nm wavelength. Measurements are taken of both

25

the 485 nm and 535 nm emission spectra, and the ratio of 535/485 nm light is a relative measure of the $[Ca^{2+}]$ within the visualized cell.   Due to photobleaching of the fluorophores over time, the data is best normalized as $\Delta R/R$ where R is the intial ratio of YFP/CFP fluorescence. Fluorescence intensities were measured using ImageJ software analysis. In my experiments, I drove expression of UAS-Cameleon in motor neurons using the motor neuron specific Gal4 driver *D42*.

Larvae were dissected in Jans buffer without calcium, as described above in the electrophysiology section. The intensity of each of channel, both FRET and CFP, was background corrected by subtracting the background from each by selecting a region surrounding each bouton that showed no specific fluorescent signal. Dividing the background corrected FRET by the CFP yielded the value R. I then gathered a control R value, R_0, by taking the average of R values from three seperate images before adding calcium. For each time point, an individual R, R_t was then calculated. ΔR is then calculated by subtracting the control R from the individual timepoint R ($R_t - R_0$). Finally, $\Delta R/R$ is calculated by dividing ΔR by the control R, R_0 (($R_t - R_0$)/R_0). This was calculated for 5 boutons per image to achieve the final $\Delta R/R$ for each timepoint per image.   n values represent the number of images averaged together. Error bars represent +/- SEM.

Chapter 3: Results

26

3.1 Drosophila mGluRA (DmGluRA) affects the rate of onset of long term facilitation (LTF), a reporter for motor neuron excitability

The observation that $mGluR^{112b}$ increases the rate of onset of LTF suggested that $DmGluRA^{112b}$ increases motor neuron excitability as well (Bogdanik et al., 2004). To confirm this suggestion, I simultaneously recorded peripheral nerve electrical activity and ejps during LTF induced by 10 Hz stimulus trains. As previously observed in the hyperexcitable genotypes described above (Ganetzky and Wu, 1982; Loughney et al., 1989; Stern and Ganetzky, 1989; Stern et al., 1990; Mallart et al., 1991; Chouinard et al., 1995; Schweers et al., 2002; Mee et al., 2004), I found that the abrupt onset of LTF in $mGluRA^{112b}$ was accompanied in the nerve by the appearance of supernumerary action potentials (Figure 3.1). This observation confirmed that LTF onset in $mGluRA^{112b}$ was caused by prolonged motor nerve terminal depolarization, and hence that $mGluRA^{112b}$ increases neuronal excitability. Thus, as suggested previously (Bogdanik et al., 2004), it appears that DmGluRA mediates an activity-dependent inhibition of neuronal excitability. In this view, glutamate release from motor nerve terminals downregulates subsequent neuronal activity by activating presynaptic DmGluRA autoreceptors, which then decrease excitability. Elimination of DmGluRA
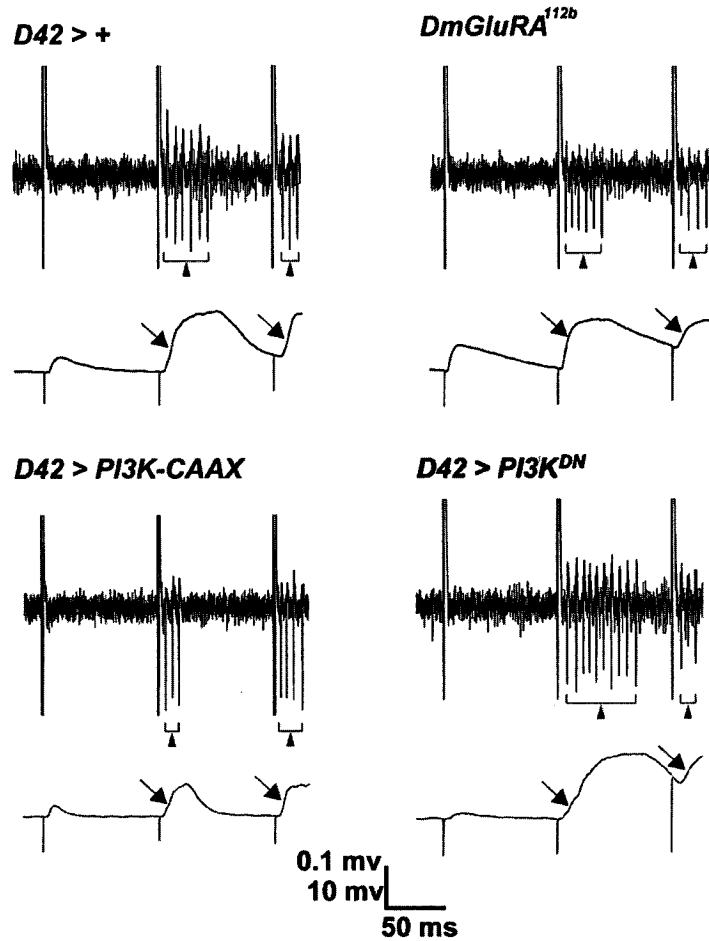
Figure 3.1. LTF onset is accompanied by supernumerary action potentials in the peripheral nerve. Simultaneous intracellular recordings from muscle (lower traces) and extracellular recordings from the innervating peripheral nerve (upper traces) in the indicated genotypes in response to 10 Hz nerve stimulation. Responses are shown immediately prior to and immediately following LTF onset. Note that LTF onset in each genotype, indicated by arrows, was accompanied by supernumerary, repetitive firing of axons in the innervating nerve (arrowheads). Bath $[Ca^{2+}]$ was 0.15 mM, quinidine concentration was 0.1 mM.

28

disrupts this negative feedback and prevents the decrease in excitability from occurring.

3.2 The DmGluRA^{112b}–null mutation increases neuronal excitability by preventing PI3K activation

In addition to increasing neuronal excitability, DmGluRA^{112b} also decreases arborization and synapse number at the larval neuromuscular junction (Bogdanik et al., 2004). This phenotype is also observed in larval motor neurons with decreased activity of PI3K (Martin-Pena et al., 2006). This observation raised the possibility that DmGluRA might exert its effects on neuronal excitability as well as synapse formation via PI3K activity. To test the possibility that PI3K mediates the effects of DmGluRA on neuronal excitability, I used the D42 Gal4 driver (Brand and Perrimon, 1993; Parkes et al., 1998) to overexpress transgenes expected to alter activity of the motor neuron PI3K pathway. I found that inhibiting the PI3K pathway by motor neuron-specific overexpression of either the phosphatase PTEN, which opposes the effect of PI3K, or the dominant-negative PI3K^{DN} (Leevers et al., 1996), each significantly increased the rate of onset of LTF, similarly to that of DmGluRA^{112b} (Figure 3.2 A and 3.2 B). In contrast, I found that activating the PI3K pathway by expression of the constitutively active

29
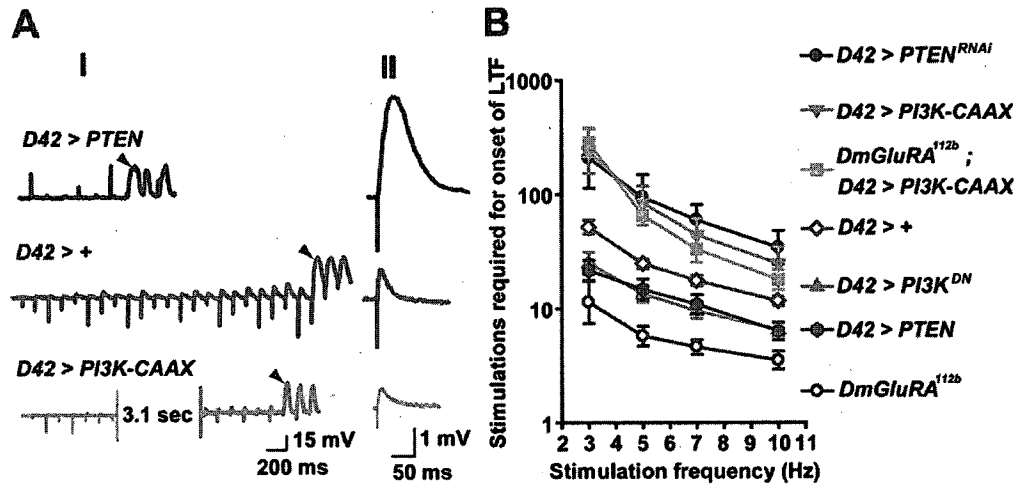
Figure 3.2. DmGluRA activity inhibits neuronal excitability via activation of the PI3K pathway. The motor neuron GAL4 driver *D42* was used to drive expression of all transgenes. For all LTF experiments, the bath solution contained 0.15 mM [Ca^{2+}] and 100 µM quinidine, which is a K^+ channel blocker that sensitizes the motor neuron and enables LTF to occur and measured even in hypoexcitable neurons. *A*, Representative traces showing the decreased rate of onset of long-term facilitation (LTF) (I) and decreased excitatory junction potential (ejp) amplitude (II) in larvae overexpressing *PI3K-CAAX* in motor neurons compared to wildtype at the indicated [Ca^{2+}], and the increased rate of onset of LTF and ejp amplitude in larvae overexpressing *PTEN*. Arrowheads indicate the increased and asynchronous ejps, indicative of onset of LTF. In (II), ejps are averages of 180 responses for each genotype. *B,* Number of stimulations required to induce LTF (Y axis) at the indicated stimulus frequencies (X axis) in the indicated genotypes. Geometric means +/- SEMs are shown. From top to bottom, *n* = 6, 12, 7, 18, 12, 21, and 6 respectively, for each genotype. One-way ANOVA and Fisher's LSD gave the following differences, at 10 Hz, 7 Hz, 5 Hz and 3 Hz, respectively: For *D42>+*: vs. *D42>PI3K-CAAX*, p=0.013, 0.0021, 0.0002, <0.0001; vs. *D42>PTEN*, p=0.011, 0.056, 0.079, 0.0054; vs. *D42>PTEN*[RNAi], p=0.0018, 0.0004, 0.0006, 0.0014; vs. *D42>PI3K*[DN], p=0.035, 0.036, 0.05, 0.038; vs. *mGluR*[112b], p=0.0012, 0.0005, 0.0004, 0.0009. For *mGluR*[112b], *D42>PI3K-CAAX* vs: *mGluR*[112b], p=0.0003, <0.0001, <0.0001, <0.0001; vs. *D42>PI3K-CAAX*, p=0.33, 0.34. 0.46, 0.62.

PI3K-CAAX (Leevers et al., 1996), or via RNAi-mediated inhibition of *PTEN*,

decreased rate of onset of LTF (Figure 3.2 A and 3.2 B). As was described

30

above for *mGluRA^{112b}*, LTF onset was accompanied by the appearance of supernumerary action potentials in the nerve (Figure 3.1) demonstrating that altered excitability is responsible for the altered rate of onset of LTF in these genotypes.

The rate of LTF onset described above was measured in the presence of the potassium channel blocking drug quinidine, which moderately increases neuronal excitability and hence rate of onset of LTF in the larval motor neuron. Quinidine application sensitizes the motor neuron to the effects of the nerve stimulation and enables LTF to occur reliably in genotypes with low excitability, even at lower stimulus frequencies. To demonstrate that altered PI3K activity does not alter rate of onset of LTF by altering sensitivity to quinidine, I compared the timing of LTF onset in the absence of quinidine in wildtype larvae and in larvae with inhibited PI3K. I found that inhibiting PI3K activity in motor neurons significantly accelerated LTF onset even in the absence of quinidine (Figure 3.3) demonstrating that altered sensitivity of motor neurons to quinidine does not underlie the altered onset rate of LTF that I observe.

In addition to effects on LTF, mutations that alter motor neuron excitability can alter basal transmitter release and hence ejp amplitude at low bath Ca^{2+} concentrations, at which Ca^{2+} influx would be limiting for vesicle fusion to occur. For example, mutations in *ether-a go-go (eag)*, which encodes a potassium

31
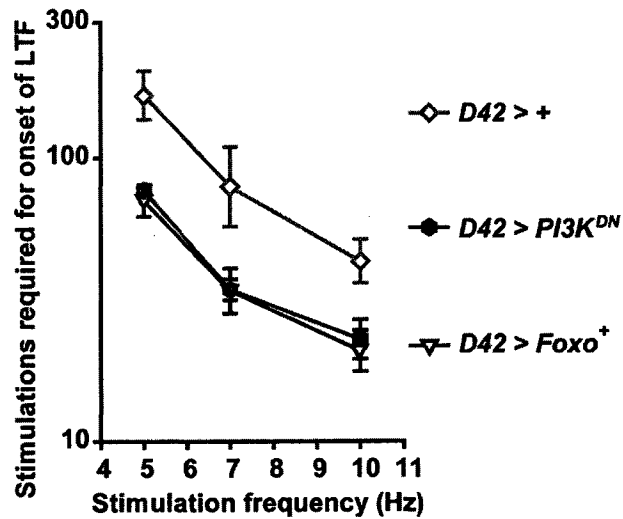
Figure 3.3: PI3K pathway inhibition increases neuronal excitability.
Number of stimulations required to induce LTF (Y axis) at the indicated
stimulus frequencies (X axis) in the indicated genotypes. Geometric means
+/- SEMs are shown. Bath [Ca^{2+}] was 0.15 mM. n=5 for all genotypes.
One-way ANOVA and Fisher's LSD gave the following differences, at 10
Hz, 7 Hz, 5 Hz respectively: For *D42>+*: vs. *D42>PI3K^{DN}*, p=0.027, 0.020,
0.0033; vs. *D42>*Foxo, p=0.0099, 0.018, <0.0001.

32

channel β-subunit, increase transmitter release about two-fold (Ganetzky and Wu, 1982), whereas a mutation in the sodium channel gene *paralytic* decreases transmitter release by increasing the frequency at which nerve stimulation failed to evoke any vesicle fusion, termed "failure" of vesicle release (Huang and Stern, 2002). Presumably altered excitability affects the amplitude or duration of the action potential and consequently the amount of Ca^{2+} influx through voltage-gated channels. I found that $DmGluRA^{112b}$ also increased ejp amplitude and hence basal transmitter release at three low bath Ca^{2+} concentrations tested (Figure 3.4 A), which is consistent with increased motor neuron excitability in this genotype. I found that decreasing PI3K pathway activity via motor neuron overexpression of $PI3K^{DN}$ or *PTEN* also increased transmitter release to levels similar to $DmGluRA^{112b}$, whereas increasing PI3K pathway activity via overexpression of *PI3K-CAAX* decreased basal transmitter release (Figure 3.4 A).

The $DmGluRA^{112b}$ mutation also decreased the frequency at which failures of vesicle release occur, particularly at the lower Ca^{2+} concentrations tested (Figure 3.4 B). This observation confirms that the effect of $DmGluRA^{112b}$ on ejp amplitude is presynaptic. I also observed a decreased frequency of failures when the PI3K pathway was inhibited by motor neuron expression of $PI3K^{DN}$ or *PTEN* (Figure 3.4 B). In contrast, motor neuron overexpression of *PI3K-CAAX* increased the frequency of failures (Figure 3.4 B). Therefore, with three electrophysiological readouts, the $DmGluRA^{112b}$ mutant phenotype was mimicked

33

A

-○- DmGluRA^{112b}

-△- D42 > PI3K^{DN}

-●- D42 > PTEN

-◇- D42 > +

-▽- D42 > PI3K-CAAX

-□- DmGluRA^{112b} ;
D42 > PI3K-CAAX

EJP amplitude (mV)

10

1

0.1

0.1 0.15 0.2
[Ca^{2+}] mM

B

-△- D42 > PI3K^{DN}

-●- D42 > PTEN

-○- DmGluRA^{112b}

-◇- D42 > +

-□- DmGluRA^{112b} ;
D42 > PI3K-CAAX

-▽- D42 > PI3K-CAAX

Succesful ejp's (%)

100

80

60

40

20

0

0.1 0.15 0.2
[Ca^{2+}] mM
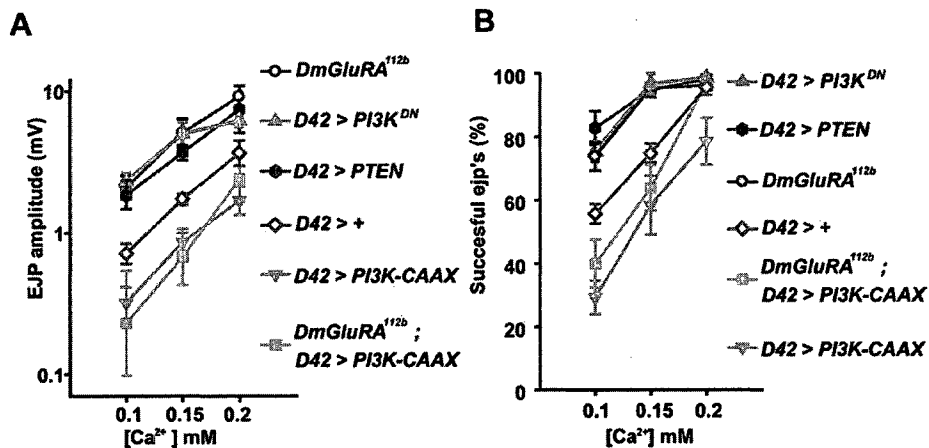
Figure 3.4. DmGluRA activity inhibits neurotransmitter release via activation of the PI3K pathway. The motor neuron GAL4 driver *D42* was used to drive expression of all transgenes. A, Mean ejp amplitudes (Y axis) at the indicated $[Ca^{2+}]$ (X axis), from the indicated genotypes. Larval nerves were stimulated at a frequency of 1 Hz, and 10 responses were measured from each of nine larvae (for *D42>PI3K-CAAX* and *D42>PI3K^{DN}*) and for six larvae from other genotypes. Means +/- SEMs are shown. One-way ANOVA and Fisher's LSD gave the following differences, at 0.1 mM, 0.15 mM and 0.2 mM $[Ca^{2+}]$, respectively: For *D42>+*: vs. *D42>PI3K-CAAX*, p=0.028, 0.05, 0.04; vs. *D42>PTEN*, p=0.017, 0.03, 0.06; vs. *D42>PI3K^{DN}*, p=0.0018, 0.0033, 0.14; vs. *mGluR^{112b}*, p=0.0077, 0.0029, 0.01. For *mGluR^{112b}*, *D42>PI3K-CAAX* vs: *mGluR^{112b}*, p<0.0001, <0.0001, 0.0001; vs. *D42>PI3K-CAAX*, p=0.70, 0.47, 0.26. B, Effects of altered PI3K pathway activity on failures of transmitter release. Mean transmitter release success rate +/- SEMs (Y axis) at the indicated Ca^{2+} concentration (X axis) for the indicated genotypes. Larval nerves were stimulated at 1 Hz. 10 responses were collected per nerve from each of 6 larvae for the given genotype and at the given Ca^{2+} concentration. One-way ANOVA and Fisher's LSD gave the following differences, at 0.1 mM, 0.15 mM and 0.2 mM $[Ca^{2+}]$, respectively: For *D42>+*: vs. *D42>PI3K-CAAX*, p=0.0023, 0.023, 0.001; vs. *D42>PTEN*, p=0.0014, 0.0068, 0.69; vs. *D42>PI3K^{DN}*, p=0.011, 0.003, 0.63; vs. *mGluR^{112b}*, p=0.027, 0.0053, 0.99. For *mGluR^{112b}*, *D42>PI3K-CAAX* vs: *mGluR^{112b}*, p=0.0001, <0.0001, 0.94; vs. *D42>PI3K-CAAX*, p=0.21, 0.45, 0.0008.

34

by decreased activity of the PI3K pathway, whereas increasing PI3K pathway activity conferred opposite effects. These observations support the notion that loss of DmGluRA increases motor neuron excitability by preventing the activation of PI3K. If so, then motor neuron expression of *PI3K-CAAX*, which will be active independently of DmGluRA, is predicted to suppress the *DmGluRA^{112b}* hyperexcitability. To test this possibility, I drove motor-neuron expression of *PI3K-CAAX* in a *DmGluRA^{112b}* background and found a rate of onset of LTF and ejp amplitude that was very similar to what was observed when *PI3K-CAAX* was expressed in a wildtype background, but significantly different from *DmGluRA^{112b}* (Figure 3.2 B, Figure 3.4 A). In addition, motor neuron-specific expression of *PI3K-CAAX* increased failure frequency at the two lower [Ca^{2+}] tested to the same level in *DmGluRA^{112b}* larvae as in wildtype (Figure 3.4 B). I conclude that hyperexcitability of the *DmGluRA^{112b}* mutant results from inability to activate PI3K.

3.3 Glutamate application increases levels of phosphorylated Akt in motor nerve terminals in a DmGluRA-dependent manner

The results described above suggest that glutamate release from motor nerve terminals as a consequence of motor neuron activity activates PI3K within motor nerve terminals via DmGluRA autoreceptors. To test this possibility directly, I measured the ability of glutamate applied to the neuromuscular junction to

35

activate PI3K within motor nerve terminals. To assay for PI3K activity I applied an antibody specific for the phosphorylated form of the kinase Akt (p-Akt), which is increased by elevated PI3K pathway activity. The usefulness of this antibody for specific detection of Drosophila p-Akt has been previously demonstrated (Colombani et al., 2005; Dionne et al., 2006; Palomero et al., 2007). The ability to detect p-Akt in larval motor nerve terminals overexpressing *PI3K-CAAX*, but not in wildtype (Figure 3.5), further validates this antibody as a PI3K reporter.

We compared p-Akt levels in wildtype versus *DmGluRA[112b]* motor nerve terminals immediately prior to or following a 1 minute application of 100 µM glutamate. I found that glutamate application strongly increased p-Akt levels in wildtype larvae, but not in the *DmGluRA[112b]* larvae (Figure 3.5), demonstrating that glutamate application increases nerve terminal p-Akt levels, and that DmGluRA activity is required for this increase.

We found that DmGluRA activity was required presynaptically for this p-Akt increase: motor neuron-specific expression of a *DmGluRA* RNAi construct (Bogdanik et al., 2004), blocked the ability of glutamate to increase p-Akt levels (Figure 3.5). In (Bogdanik et al., 2004) it was reported that expression of *DmGluRA* RNAi decreased, but did not eliminate, mGluRA immunoreactivity, suggesting that this transgene decreases, but does not eliminate, glutamate-mediated signalling via mGluRA. The ability of this transgene to block glutamate-mediated induction of p-Akt suggests that activation of PI3K by glutamate is sensitive to mGluRA levels and requires a minimum level of mGluRA expression. In contrast, expression of the *DmGluRA*

36

RNAi construct in the muscle, with use of the *24B Gal4* driver, did not inhibit p-Akt levels: p-Akt intensity following 1 minute of glutamate application was not significantly different from wildtype (17.6 +/- 2.9, p=0.59).

To determine if PI3K activity was required presynaptically for this glutamate-induced p-Akt increase, I inhibited PI3K activity by motor neuron-expression of *PI3K^{DN}*, and found that this transgene significantly inhibited the ability of glutamate to activate p-Akt (Figure 3.5). Thus, presynaptic DmGluRA and PI3K activity are both necessary for glutamate to increase p-Akt.

3.4 The effects of PI3K on neuronal excitability are mediated by Foxo, not Tor/S6 Kinase

Many effects of the PI3K pathway are mediated by the downstream kinase Akt. Activated Akt phosphorylates targets such as Tsc1/Tsc2, which regulates cell growth via the Tor/S6 Kinase (S6K) pathway (Hay and Sonenberg, 2004), Foxo, which regulates apoptosis (Tang et al., 1999), and GSK3 (Cross et al., 1995), which mediates at least in part the effects of altered PI3K pathway activity on arborization and synapse number (Martin-Pena et al., 2006). All of these Akt-mediated phosphorylation events inhibit activity of the target protein. If PI3K pathway activity decreases neuronal excitability by inhibiting Foxo, then Foxo
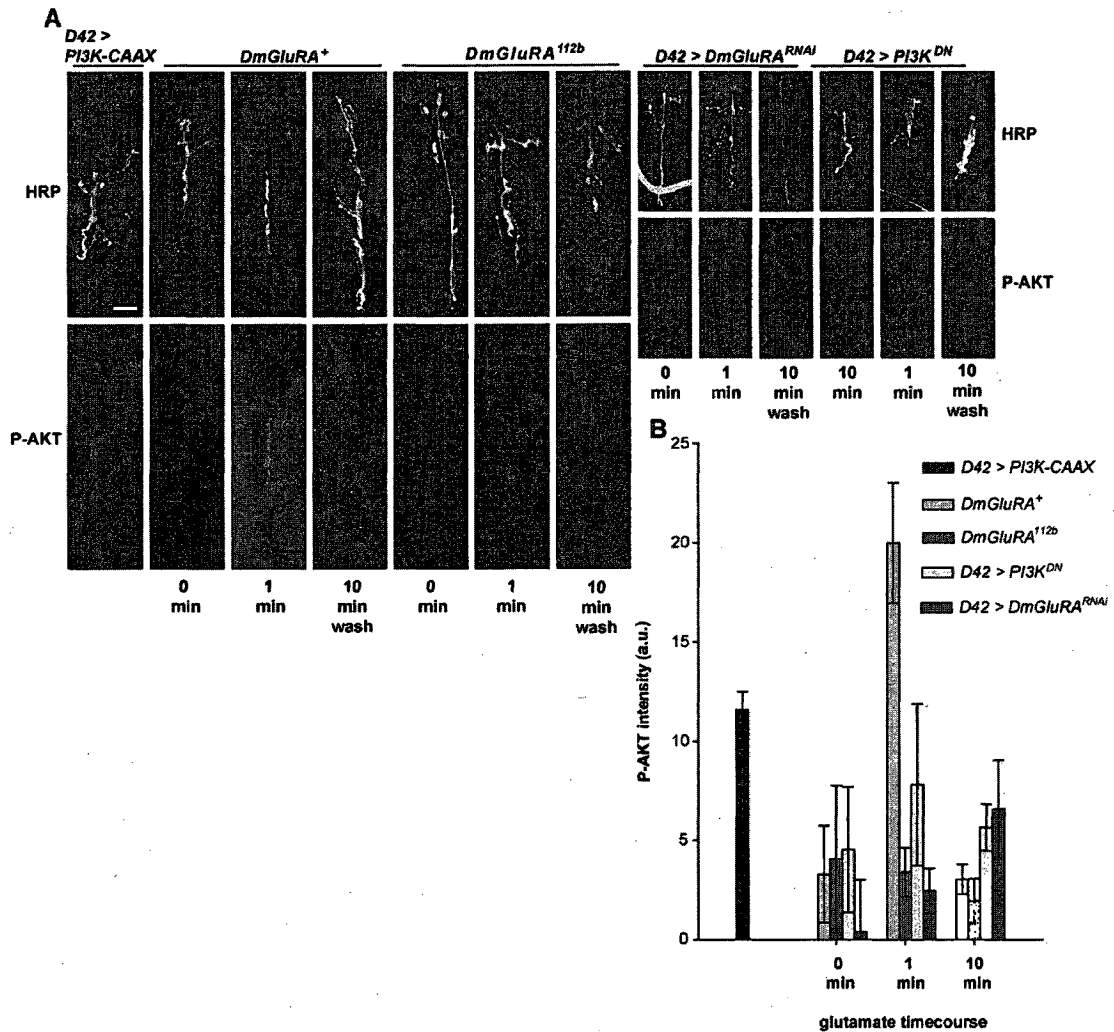
Figure 3.5. Glutamate application stimulates presynaptic Akt phosphorylation in
$DmGluRA^+$ but not in $DmGluRA^{112b}$ mutant larvae. *A*, Representative confocal images
of $DmGluRA^+$, $DmGluRA^{112b}$, $D42{>}DmGluRA^{RNAi}$ and $D42{>}PI3K^{DN}$ larvae stained with
anti-HRP (upper) and anti-p-Akt (lower) in the indicated conditions. All images are from
muscles 7 and 6 of abdominal segment A3 or A4. Scale bar = 20 μm. *B*, Quantification
of phosphorylated Akt (p-Akt) levels in $DmGluRA^+$, $DmGluRA^{112b}$, $D42{>}DmGluRA^{RNAi}$
and $D42{>}PI3K^{DN}$ larvae immediately prior to glutamate application, after 1 min of 100
μM glutamate application (final bath concentration), and 10 min after a wash with
glutamate free media. Nerve terminals were outlined with HRP fluorescence as
reference. Pixel intensities were quantified using ImageJ software and background
subtraction was performed as described in detail in Methods section. Bars represent
mean synaptic p-Akt levels +/- SEMs. *D42 > PI3K-CAAX* is included as a positive
control. One-way ANOVA and Fisher's LSD gave the following significant differences
for p-Akt levels one minute after glutamate application. For $DmGluRA^+$ vs.
$DmGluRA^{112b}$, p=0.0072; vs. $D42{>}PI3K^{DN}$, p=0.0097; vs. $D42{>}DmGluRA^{RNAi}$, p<0.0001.

38

overexpression is predicted to mimic the hyperexcitability observed when PI3K pathway activity is blocked in motor neurons, whereas loss of Foxo is predicted to mimic the hypoexcitability observed when *PI3K-CAAX* is expressed in motor neurons. To test these predictions, I measured neuronal excitability in larvae carrying the heteroallelic *Foxo[21]/Foxo[25]* null mutant combination (Junger et al., 2003) and in larvae overexpressing *Foxo[+]* (Hwangbo et al., 2004) in motor neurons. I found that overexpression of *Foxo[+]* increased the rate of onset of LTF, basal transmitter release and frequency of successful ejps to a level very similar to that observed when PI3K pathway activity was decreased (Figure 3.6) whereas in *Foxo[21]/Foxo[25]* larvae, the rate of onset of LTF, basal transmitter release and frequency of successful ejps were decreased to levels very similar to those observed when *PI3K-CAAX* was expressed in motor neurons (Figure 3.6). These observations support the notion that PI3K activity decreases excitability by downregulating Foxo activity.

If the hyperexcitability conferred by motor neuron expression of *PI3K[DN]* results from Foxo hyperactivity, then the *Foxo[21]/Foxo[25]* null combination will suppress this hyperexcitability and confer motor neuron hypoexcitability similar to what is observed in *Foxo[21]/Foxo[25]* larvae in an otherwise wildtype background. I confirmed this prediction: larvae carrying the *Foxo[21]/Foxo[25]* null combination and expressing *PI3K[DN]* in motor neurons exhibited a rate of onset of LTF, basal transmitter release, and failure frequency very similar to what was observed in the *Foxo[21]/Foxo[25]* null mutant alone (Figure 3.6), or in larvae expressing *PI3K-*

A

I

D42 > FOXO

D42 > +

Foxo²¹/Foxo²⁵

2.7 sec

$\rfloor$15 mV
200 ms

II

$\rfloor$1 mV
50 ms

B

- D42 > PI3K-CAAX
- Foxo²¹/Foxo²⁵
- Foxo²¹/Foxo²⁵; OK6 > PI3K^{DN}
- D42 > +
- D42 > PI3K-CAAX; Foxo⁺
- D42 > PI3K^{DN}
- OK6 > PI3K^{DN}
- D42 > Foxo⁺

Stimulations required for onset of LTF

Stimulation frequency (Hz)

C

EJP amplitude (mV)

[Ca²⁺] mM

- D42 > Foxo⁺
- D42 > PTEN
- D42 > PI3K-CAAX; Foxo⁺
- D42 > +
- D42 > PI3K-CAAX
- Foxo²¹/Foxo²⁵; OK6 > PI3K^{DN}
- Foxo²¹/Foxo²⁵

D

Succesful ejp's (%)

[Ca²⁺] mM

- D42 > Foxo⁺
- D42 > PI3K^{DN}
- D42 > PTEN
- D42 > PI3K-CAAX; Foxo⁺
- D42 > +
- D42 > PI3K-CAAX
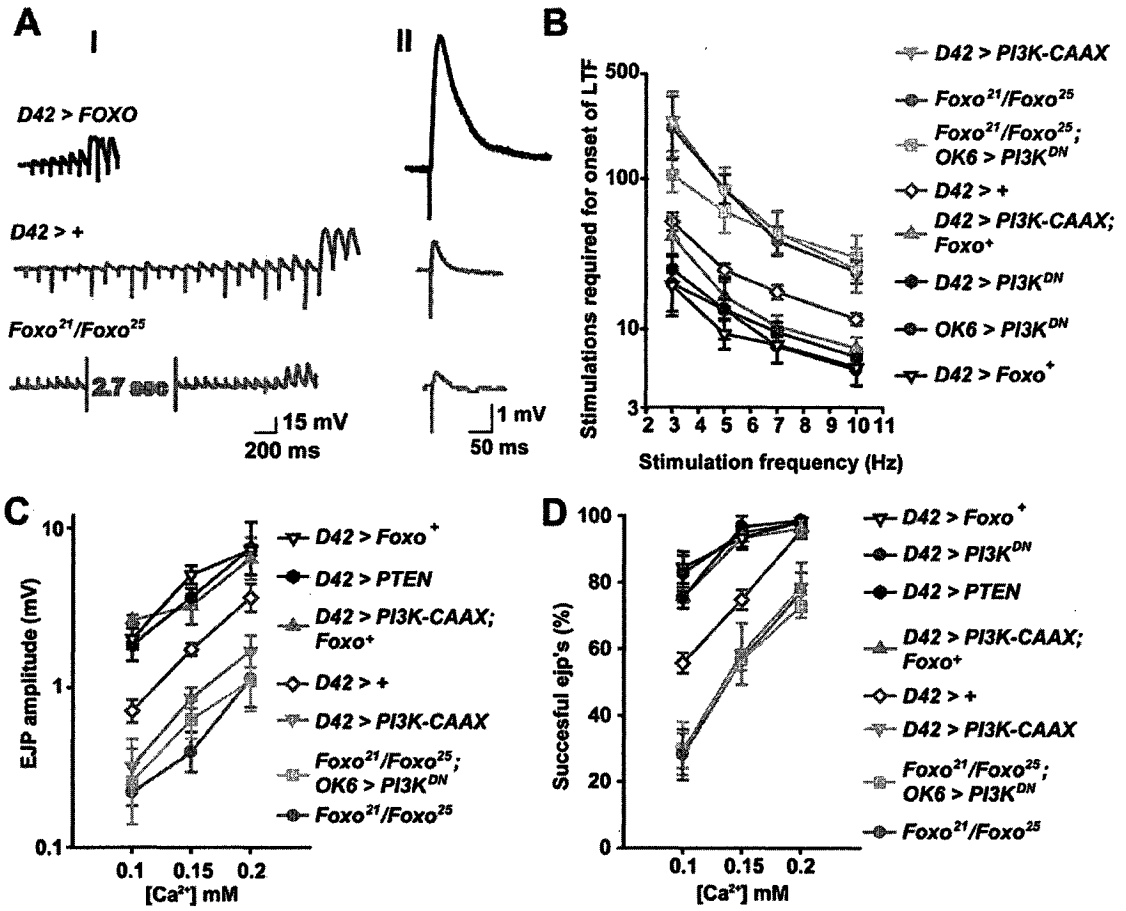- Foxo²¹/Foxo²⁵; OK6 > PI3K^{DN}
- Foxo²¹/Foxo²⁵

40

Figure 3.6. Foxo mediates the effects of PI3K on motor neuron excitability. The *Gal4* driver *D42* was used to drive expression of transgenes in all genotypes except for *Foxo²¹/Foxo²⁵; OK6>PI3K^{DN}*, in which the motor neuron driver *OK6* was used and which behaves similarly to *D42* in this assay. For all LTF experiments, the bath solution contained 0.15 mM [Ca^{2+}] and 100 μM quinidine. A, Representative traces showing the decreased rate of onset of LTF (I) and decreased ejp amplitude (II) in *Foxo²¹/Foxo²⁵* larvae compared to wildtype at the indicated [Ca^{2+}], and the increased rate of onset of LTF and ejp amplitude in larvae overexpressing *Foxo*. Arrowheads indicate the increased and asynchronous ejps, indicative of onset of LTF. In (II), representative traces are averages of multiple ejps. From *top* to *bottom*, n = 23, 180, and 34 respectively. B, Number of stimulations required to induce LTF (Y axis) at the indicated stimulus frequencies (X axis). Geometric means +/- SEMs are shown. From *top* to *bottom*, n = 12, 6, 7, 18, 10, 21, 5, and 9 respectively, for each genotype. One-way ANOVA and Fisher's LSD gave the following differences, at 10 Hz, 7 Hz, 5 Hz and 3 Hz, respectively: For *D42>+* vs. *Foxo²¹/Foxo²⁵*, p= 0.0096, 0.0069, <0.0001, 0.0007; vs. *D42>Foxo⁺*, p=0.0026, 0.0012, <0.0001, 0.0065. For *D42>PI3K-CAAX, Foxo* vs. *D42>PI3K-CAAX*, p=0.0041, 0.0005, 0.0002, 0.0006; vs. *D42>Foxo*, p=0.50, 0.43, 0.16, 0.14. For *Foxo²¹Foxo²⁵; OK6>PI3K^{DN}* vs. *OK6>PI3K^{DN}*, p=; 0.0003, 0.0004, 0.0014, 0.001. vs. *Foxo²¹Foxo²⁵*, p=0.63, 0.74, 0.43, 0.20. C, Mean ejp amplitude +/- SEMs (Y axis) for each genotype at the indicated [Ca^{2+}]. Nerves from six larvae were stimulated at a frequency of 1 Hz, and 10 responses were measured per larva. One-way ANOVA and Fisher's LSD gave the following differences, at 0.1 mM, 0.15 mM and 0.2 mM [Ca^{2+}], respectively: For *D42>+* vs. *Foxo²¹/Foxo²⁵*, p=0.0079, <0.0001, 0.012; vs. *D42>Foxo*, p=0.017, 0.0005, 0.10. For *Foxo²¹/Foxo²⁵; OK6>PI3K^{DN}*: vs. *Foxo²¹/Foxo²⁵*, p=0.74, 0.12, 0.93; vs. *D42>PI3K^{DN}*, p<0.0001, <0.0001, 0.0001; vs. *D42>PTEN*, p<0.0001, <0.0001, <0.0001. For *D42>PI3K-CAAX, Foxo* vs. *D42>PI3K-CAAX*, p<0.0001, <0.0001, =0.0024; vs. *D42>Foxo*, p=0.52, 0.13, 0.77. D, Mean transmitter release success rate +/- SEMs (Y axis) at the indicated Ca^{2+} concentration (X axis) for the indicated genotypes. Larval nerves were stimulated at 1 Hz. 10 responses were collected per nerve from each of 6 larvae for the given genotype and at the given Ca^{2+} concentration. One-way ANOVA and Fisher's LSD gave the following differences, at 0.1 mM, 0.15 mM and 0.2 mM [Ca^{2+}], respectively: For *D42>+* vs. *Foxo²¹/Foxo²⁵*, p=0.0008, 0.0039, 0.0009; vs. *D42>Foxo*, p=0.0008, 0.004, 0.7. For *Foxo²¹/Foxo²⁵; OK6>PI3K^{DN}*: vs. *Foxo²¹/Foxo²⁵*, p=0.81, 0.99, 0.43. vs. *D42>PI3K^{DN}*, p<0.0001, <0.0001, <0.0001. vs. *D42>PTEN*, p<0.0001, <0.0001, <0.0001. For *D42>PI3K-CAAX, Foxo* vs. *D42>PI3K-CAAX*, p<0.0001, <0.0001, =0.002; vs. *D42>Foxo*, p=0.29, 0.98, 0.7.

41

CAAX in motor neurons. I used the *OK6* motor neuron *Gal4* driver rather than *D42* for ease of stock construction in experiments involving *Foxo²¹/Foxo²⁵*. *OK6* confers motor neuron phenotypes indistinguishable from *D42* in my assays (Figure 3.6 B and not shown).

In addition, if the hypoexcitability conferred by motor neuron expression of *PI3K-CAAX* results from decreased Foxo activity, then co-overexpression of *Foxo⁺* will suppress this hypoexcitability and confer hyperexcitability similar to what is observed when *PI3K^{DN}*, *PTEN* or *Foxo⁺* alone are expressed in motor neurons. I confirmed this prediction: larvae co-expressing *Foxo⁺* and *PI3K-CAAX* in motor neurons exhibited rate of onset of LTF, basal transmitter release and failure frequency very similar to what was observed when *PI3K^{DN}*, *PTEN,* or *Foxo⁺* alone were expressed in motor neurons (Figure 3.6). Thus, eliminating *Foxo* reverses the hyperexcitability conferred by blocking PI3K pathway in motor neurons, whereas overexpressing *Foxo⁺* reverses the hypoexcitability confered by activating PI3K in motor neurons. These epistasis tests support the notion that PI3K activity decreases motor neuron excitability by inhibiting Foxo.

In contrast, I found that altering the Tor/S6K pathway had little effect on motor neuron excitability. In particular, motor neuron expression of neither the dominant-negative *S6K^{DN}* nor the constitutively active *S6K^{Act}* transgene (Barcelo and Stewart, 2002) had any effect on the rate of onset of LTF (Figure 3.7). In addition, except for the appearance of some enhancement at the lowest stimulus frequency applied, expression of *S6K^{DN}* had no effect on the ability of *PI3K-*

42

CAAX to decrease the rate of onset of LTF (Figure 3.7). Furthermore,

expression of *S6K^{DN}* had no effect on basal transmitter release, and did not affect

the ability of *PI3K-CAAX* to depress basal transmitter release (data not shown).

Therefore I conclude that the Tor/S6K pathway does not mediate the effects of

PI3K on neuronal excitability.

3.5 The effects of PI3K on neuronal growth are mediated by Tor/S6 Kinase, not Foxo

3.5.1   Nerve terminal growth

Because altered PI3K pathway activity alters motor neuron arborization and

synapse number (Martin-Pena et al., 2006), it seemed possible that a causal

relationship existed between the PI3K-mediated excitability and neuroanatomy

defects. To test this possibility, I evaluated the roles of the Tor/S6K and Foxo

pathways in mediating the effects of altered PI3K activity on synapse number. I

found that motor neuron-specific expression of *S6K^{Act}* increased synapse number

to an extent similar to *PI3K-CAAX,* and motor neuron expression of *S6K^{DN}*

partially suppressed the increase in synapse number conferred by *PI3K-CAAX*

(Figure 3.8 A and 3.8 B). These observations suggest that S6K mediates in part

the effects of PI3K on arborization and synapse number. However, the ability of

43
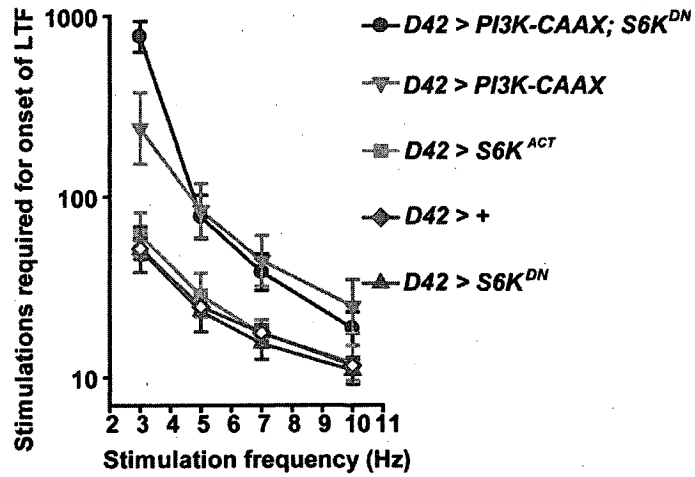
Figure 3.7. *S6K* does not mediate the effects of *PI3K* on motor neuron excitability. Number of stimulations required to induce LTF (Y axis) at the indicated stimulus frequencies (X axis). The bath solution contained 0.15 mM $[Ca^{2+}]$ and 0.1 mM quinidine. Geometric means +/- SEMs are shown. From *top* to *bottom*, n = 12, 7, 9, 14, and 18 respectively, for each genotype.

44

S6K^{DN} to suppress only partially the effects of PI3K-CAAX overgrowth suggests that both Tor/S6K and a second, PI3K-mediated, pathway (presumably involving GSK3) regulate synapse formation. A role for the Tor/S6K in the control of synapse number was previously reported by Knox et al. (2007). In this report, null mutations in *S6K* decreased synapse number as well as muscle size at the larval nmj. However, it was further reported that activation of the PI3K effector Rheb, which activates Tor/S6K, increased synapse number at the larval nmj even when Tor activity was inhibited by rapamycin (Knox et al., 2007), raising the possibility that Rheb activates synapse formation via multiple redundant pathways, including Tor/S6K. In contrast to the effects of altered S6K on synapse formation, I found that *Foxo*$^{+}$ overexpression had no effect on synapse number (data not shown) and failed to suppress the growth-promoting effects of PI3K-CAAX (Figure 3.8 A and 3.8 B).

3.5.2   Axon diameter

We found that the PI3K pathway also affects axon diameter. In Drosophila peripheral nerves, about 80 axons, including about 35 motor axons, are wrapped by about three layers of glia, as shown in the transmission electron micrograph from cross sections of peripheral nerves in Figure 3.8 C. I found that motor neuron specific expression of *PTEN* decreased motor axon diameter, whereas

45
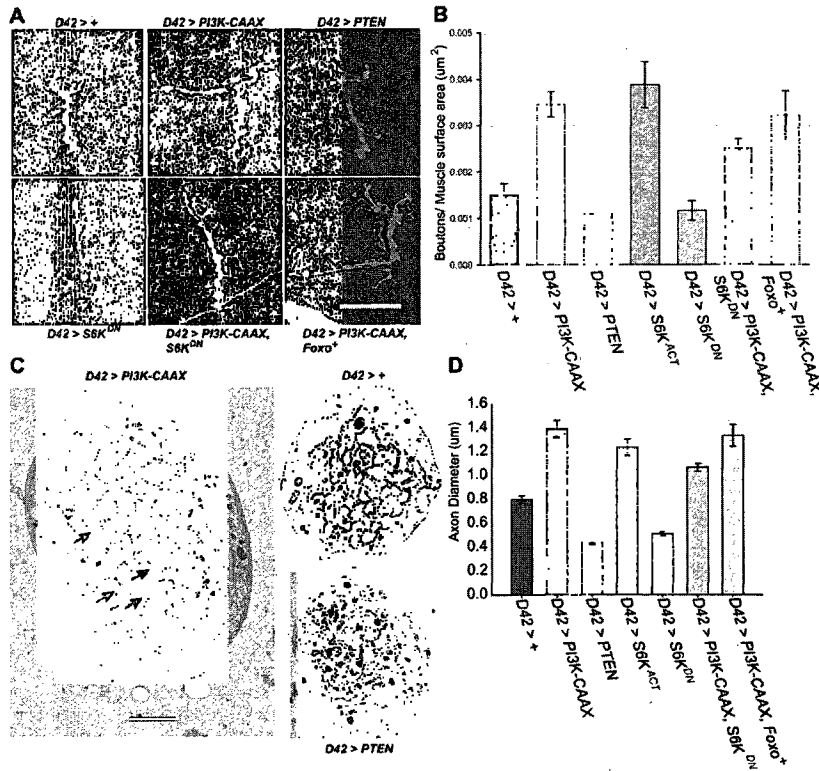
Figure 3.8. PI3K regulates synapse formation and axon growth via S6K, not Foxo. *A,* Representative images of muscles 7 and 6 in the indicated genotypes. Larva were stained with anti-HRP (green). Scale bar = 50 μm. *B,* Mean number (+/- S.E.M.s) of synaptic boutons normalized to the surface area of muscle 6 at abdominal segment A3 in the indicated genotypes. From left to right, n=6, 8, 6, 6, 7, 11, 11, respectively, for each genotype. One-way ANOVA and Fisher's LSD gave the following differences: For *D42>S6K^{Act}* vs. *D42>PI3K-CAAX*, p=0.40; vs. *D42>+*, p=0.0009. For *D42>PI3K-CAAX* vs. *D42>PI3K-CAAX, Foxo*, p=0.64; vs. *D42>PI3K-CAAX, S6K^{DN}*, p=0.05. *C,* Representative transmission electron micrographs of peripheral nerve cross sections. Axons are marked with arrows. Scale bar = 2 μm. *D,* Mean axon diameter (+/- S.E.M.s) of the five largest axons from five different nerves (25 measurements total) for the indicated genotypes. One-way ANOVA and Fisher's LSD gave the following significant differences: for *D42>+*: vs. *D42>PI3K-CAAX*, $p<0.0001$; vs. *D42>PTEN*, $p<0.0001$; vs. *D42>S6K^{DN}*, p=0.0009; vs. *D42>S6K^{act}*, $p<0.0001$; vs. *D42>PI3K-CAAX, Foxo*, $p<0.0001$; vs *D42>PI3K-CAAX, S6K^{DN}*, p=0.0011. For *D42>PI3K-CAAX* vs. *D42>PI3K-CAAX, S6K^{DN}*, p=0.0002. Means from *D42>PI3K-CAAX* and *D42>PI3K-CAAX, Foxo* were judged to be not significantly different (p=0.43). Confocal images for arborization measurements captured in part by Curtis Lin. All samples for electron microscopy were prepared by and electron micrographs captured by William Lavery.

46

motor-neuron specific expression of *PI3K-CAAX* increased motor axon diameter. Tor/S6K, but not Foxo, mediates this growth effect. In particular, motor neuron-specific expression of *S6K*^{Act} increased axon diameter to an extent similar to *PI3K-CAAX*, and motor-neuron-specific expression of *S6K*^{DN} decreased motor axon diameter to an extent similar to *PTEN* and also partially suppressed the growth-promoting effects conferred by *PI3K-CAAX*. In contrast, *Foxo*$^{+}$ overexpression did not have a significant effect on the ability of PI3K-CAAX to increase axon diameter (Figure 3.8 D). Therefore, Foxo mediates the excitability effects, but not the growth-promoting effects, of altered PI3K pathway activity, whereas the Tor/S6K pathway mediates in part the growth promoting effects but not the excitability effects of altered PI3K pathway. I conclude that the excitability and growth effects are completely separable genetically and thus have no causal relationship.

3.6 Activity-Dependent Increase in synapse number requires PI3K activity

Depending on the system, neuronal activity can either restrict or promote synapse formation (Vicario-Abejon et al., 2002). The Drosophila *eag Sh* double mutant, in which two distinct potassium channel subunits are simultaneously disrupted, displays extreme neuronal hyperexcitability (Ganetzky and Wu, 1982), and a consequent increase in synapse number (Budnik et al., 1990; Davis et al., 1996). This activity-dependent increase in

47

synapse number does not require DmGluRA activity (Bogdanik et al., 2004), suggesting that excessive glutamate release is not necessary for this excessive growth to occur. To determine if PI3K activity is required for this overgrowth, I compared synapse number in wildtype larvae, in larvae expressing dominant-negative transgenes for both *eag* (*eag^{DN}*) and *Sh* (*Sh^{DN}*) (Broughton et al., 2004; Mosca et al., 2005) in motor neurons, and in larvae co-expressing *eag^{DN}*, *Sh^{DN}* and *PI3K^{DN}*. I found that co-expression of *eag^{DN}* and *Sh^{DN}* in motor neurons increased synapse number similarly to what was observed previously (Budnik et al., 1990), and that this increase was completely blocked by simultaneous expression of *PI3K^{DN}* but not by *lacZ* (Figure 3.9). Thus, the activity-dependent increase in synapse formation requires PI3K activity. The observation that glutamate activation of DmGluRA is not necessary for this increase raises the possibility that another PI3K activator contributes to synapse formation at the larval nmj. Insulin is a plausible candidate for such an activator because both insulin and insulin receptor immunoreactivity are present at the nmj (Gorczyca et al., 1993).

48
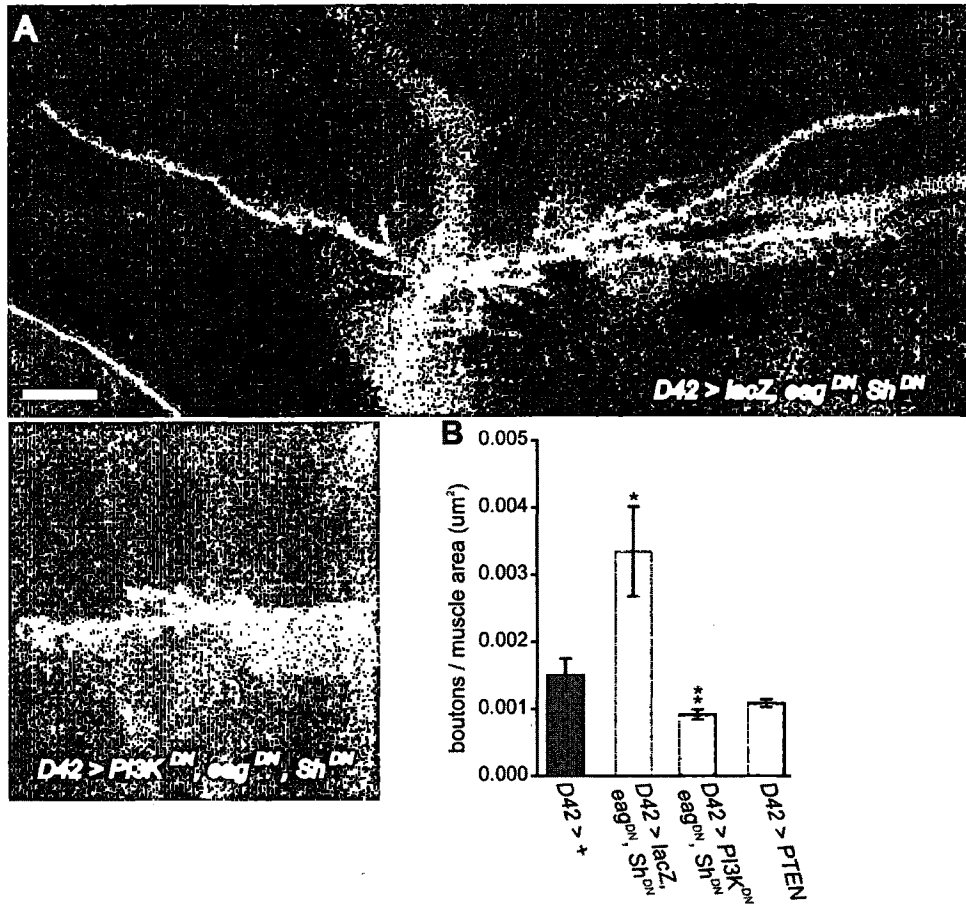
Figure 3.9. $PI3K^{DN}$ *expression suppresses the synaptic overgrowth conferred by motor neuron expression of* eag^{DN} *and* Sh^{DN}. *The* D42 Gal4 driver was used to induce motor neuron transgene expression. *A,* Representative confocal images of muscles 7 and 6 in the indicated genotypes. Larvae were stained with anti-HRP (green). Scale bar = 20 μm. *B,* Mean number (+/- S.E.M.s) of synaptic boutons normalized to the surface area (Y axis) of muscle 6 at abdominal segment A3 in the indicated genotypes (X axis). From *top* to *bottom, n* = 12, 6, 6 and 6 respectively, for each genotype. One-way ANOVA and Fisher's LSD gave the following differences: For *D42>lacZ, eag*^{DN}, *Sh*^{DN} vs. *D42>+,* p=0.027; vs. *D42>PI3K*^{DN}, *eag*^{DN}, *Sh*^{DN}, p=0.0075. For *D42>PI3K*^{DN}, *eag*^{DN}, *Sh*^{DN} vs. *D42>PTEN,* p=0.86

49

3.7 Drosophila Homer regulates neuronal excitability via a non-DmGluRA dependant mechanism

Mammalian group I mGluRs activate PI3K via the Homer scaffolding protein and the PI3K enhancer PIKE (Rong et al., 2003) thus making Homer an attractive candidate to mediate DmGluRAs activation of PI3K. In addition, Drosophila *Homer* mutants exhibit defects in locomotor control (Diagana et al., 2002) a phenotype that can be associated with defects in synaptic transmission (Stern and Ganetzky, 1989; Stern et al., 1990; Huang and Stern, 2002). This hypothesis becomes problematic, however, when it is considered that Drosophila mGluRA, similar to mammalian group II mGluRs, lacks a Homer binding motif (Diagana et al., 2002). Since Drosophila only contain one known mGluR gene, it remains possible, however, that they have evolved an alternative mechanism by which DmGluRA can interact with Homer and thus lead to PI3K activation. Another pitfall of this hypothesis is that while Drosophila Homer has been shown to be located in the dendrites and endoplasmic reticulum (ER) of motor neurons (Diagana et al., 2002), its presence at motor nerve terminals has not been shown. Based on this evidence it is unclear whether Drosophila Homer mediates activation of the PI3K pathway by DmGluRA at motor nerve terminals.

If DmGluRA activates PI3K via a Homer scaffolding complex, then loss of Homer is predicted to mimic the hyperexcitability observed when DmGluRA activation of PI3K is blocked in motor neurons (Figure 3.2, and Figure 3.4),

50

whereas Homer overexpression is predicted to mimic the hypoexcitability observed when *PI3K-CAAX* is expressed in motor neurons (Figure 3.2, and Figure 3.4). To test these predictions, I measured neuronal excitability in larvae carrying the *Homer^{R102}* null mutation (Diagana et al., 2002) and in larvae overexpressing a wildtype *Homer* transgene (*EP-Homer*) in motor neurons. I found that in *Homer^{R102}* mutant larvae, the rate of onset of LTF was increased to a level very similar to that observed when activation of PI3K pathway activity was blocked by the *DmGluRA^{112b}* null mutation (Figure 3.10 A) whereas when *EP-Homer* was overexpressed, the rate of onset of LTF was decreased to levels very similar to those observed when *PI3K-CAAX* was expressed in motor neurons (Figure 3.10 A).

If Drosophila Homer acts as an intermediate in the process of DmGluRA activation of PI3K it is also predicted that *Homer^{R102}* mutant larvae would exhibit a suppression of the glutamate induced P-AKT increase observed in wildtype larvae (Figure 3.5), similar to the phenotype of *DmGluRA^{112b}* larvae. When I tested this hypothesis, however, I found that *Homer^{R102}* mutants exhibited a wildtype P-AKT response (Figure 3.10 B)

Together, these results suggest that Homer may be an important regulator of neuronal excitability in Drosophila. However, this regulation appears to be independent of the DmGluRA-PI3K pathway described in this thesis. Further experimentation will be required to elucidate this role.

51

A

B

glutamate timecourse
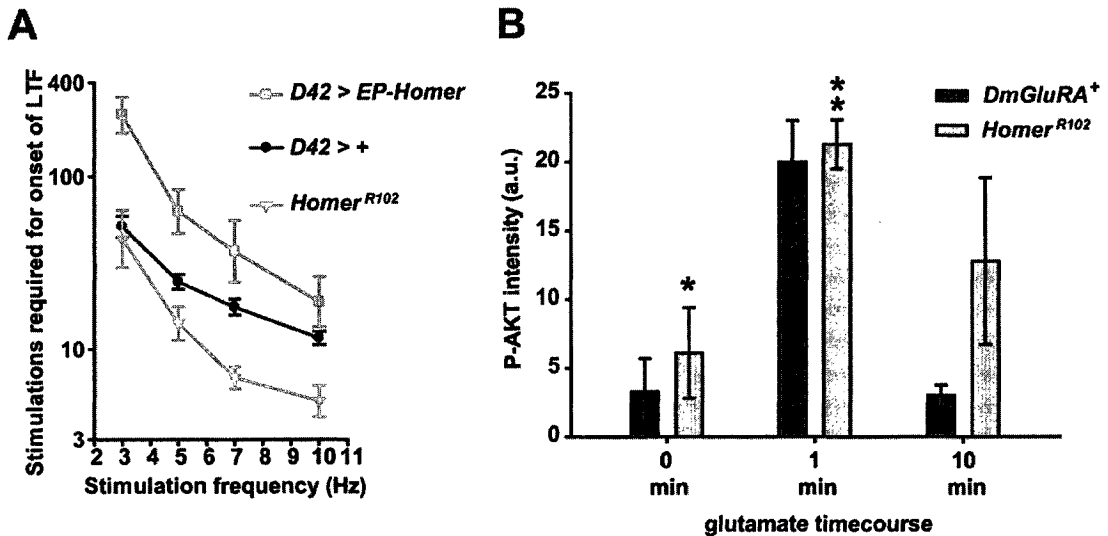
*Figure 3.10 Homer regulates neuronal excitability via a DmGluRA
independent mechanism.* A, Quantification of the rate of onset of long term
facilitation for each genotype. The bath $[Ca^{2+}]$ was 0.15 mM. A 100 µM
concentration of quinidine was present in the recording solution. The
geometric mean of number of stimulations required for the onset of long-term
facilitation at the indicated stimulus frequencies is shown for each genotype.
From *top* to *bottom*, n = 6, 18, and 7, respectively, for each genotype. Error
bars represent SEMs. B, Quantification of phosphorylated Akt (p-Akt) levels
in *DmGluRA+*, and *Homer^{R102}* larvae immediately prior to glutamate
application, after 1 min of 100 µM glutamate application (final bath
concentration), and 10 min after a wash with glutamate free media. Nerve
terminals were outlined with HRP fluorescence as reference. Pixel intensities
were quantified using ImageJ software and background subtraction was
performed as described in detail in Methods section. Bars represent mean
synaptic p-Akt levels +/- SEMs. The P-AKT experiment was conducted in
large part by Elaina Bolinger.

52

3.8 Retrograde transport required for proper regulation of synaptic transmission:

According to my model, Akt activated by phosphorylation at the synapse targets the transcription factor Foxo in order to regulate synaptic transmission. In order for p-Akt to interact with Foxo, I hypothesize that p-Akt undergoes retrograde transport from the synapse to the nucleus. To test this hypothesis, I expressed a dominant negative dynactin transgene ($Glued^{DN}$ (Allen et al., 1999)) in motor neurons which interferes with retrograde axonal transport. As expected, I observed a drastic increase in both the rate of onset of LTF (Figure 3.11) and in basal transmitter release (data not shown). my model would suggest these electrophysiological effects to be due to the relief of inhibition of Foxo by p-Akt, thus allowing Foxo to promote excitability unencumbered. Alternatively, the observed results could be caused by an unrelated and unknown developmental defect since disruption of Glued is known to affect synapse formation in ways not described by my model (Eaton et al., 2002; Morales-Mulia and Scholey, 2005; Vendra et al., 2007)

53
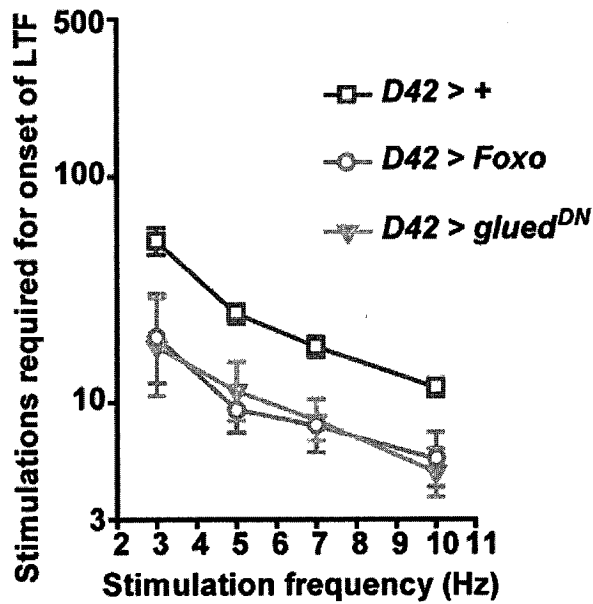
Figure 3.11. Retrograde axonal transport required for proper regulation of synaptic transmission. Quantification of the rate of onset of long term facilitation for each genotype. The bath $[Ca^{2+}]$ was 0.15 mM. A 100 μM concentration of quinidine was present in the recording solution. The geometric mean of number of stimulations required for the onset of long-term facilitation at the indicated stimulus frequencies is shown for each genotype. From *top* to *bottom*, *n* = 18, 9, and 5, respectively, for each genotype. Error bars represent SEMs.

54

3.9 DmGluRA activity initiates an increase in Ca^{2+} within nerve terminals

Another attractive candidate for an intermediate between Drosophila mGluR and PI3K is Ca^{2+} signaling via the release of Ca^{2+} from internal stores. Ca^{2+} increases can lead to the release of insulin, which could in turn lead to the activation of PI3K. mGluRs induce postsynaptic long term depression (LTD) in mammals (Bashir et al., 1993); a process dependant on an increase in intracellular calcium (Lynch et al., 1983). These mGluR dependant Ca^{2+} increases are dependent on two Ca^{2+} sensing molecules, protein interacting with C kinase (PICK1) and neuronal Ca^{2+} sensor (NCS-1) in addition to IP3 (Jo et al., 2008). NCS-1, and its Drosophila homolog frequenin, can act to regulate the release of Ca^{2+} from internal stores via activation of the inositol 1,4,5-trisphosphate receptor (IP3R), yet can also be regulated by the surrounding [Ca^{2+}] (Choe and Ehrlich, 2006). Since PICK1 has been shown to bind and interact with the C-terminal of group II mGluRs, it remains possible that an interaction between DmGluRA and the Drosophila homolog of PICK1 could occur.

Taken together, the findings discussed in the above paragraph raise the possibility that DmGluRA activity initiates an increase in intracellular Ca^{2+} levels in the nerve terminal. To test this possibility directly, I measured the ability of glutamate applied to the neuromuscular junction to initiate an increase in Ca^{2+} levels within motor nerve terminals. To assay for changes in Ca^{2+} I drove

55

expression of a Förster resonance energy transfer (FRET)-based Ca^{2+} sensor transgene (UAS-Cameleon) specifically within nerve terminals.

We compared FRET signal intensity levels in wildtype versus $D42>DmGluRA^{RNAi}$ motor nerve terminals immediately prior to or every 5 seconds for a minute after application of 100 μM glutamate. Subsequent measurements were taken every minute following for a total of five minutes of recording. I found that glutamate application strongly increased FRET-signal intensity in wildtype larvae, but not in the $DmGluRA^{RNAi}$ larvae (Figure 3.12), demonstrating that glutamate application increases nerve terminal Ca^{2+} levels, and that DmGluRA activity is required for this increase.

While $DmGluRA^{RNAi}$ larvae did not respond immediately to the addition of glutamate, the larvae did exhibit a Ca^{2+} increase 2 minutes after the initial addition of glutamate (Figure 3.12). This could represent a non-mGluR dependent mechanism by which glutamate can induce changes in intracellular Ca^{2+} levels within the nerve terminal, presumably by ionotropic glutamate receptors.
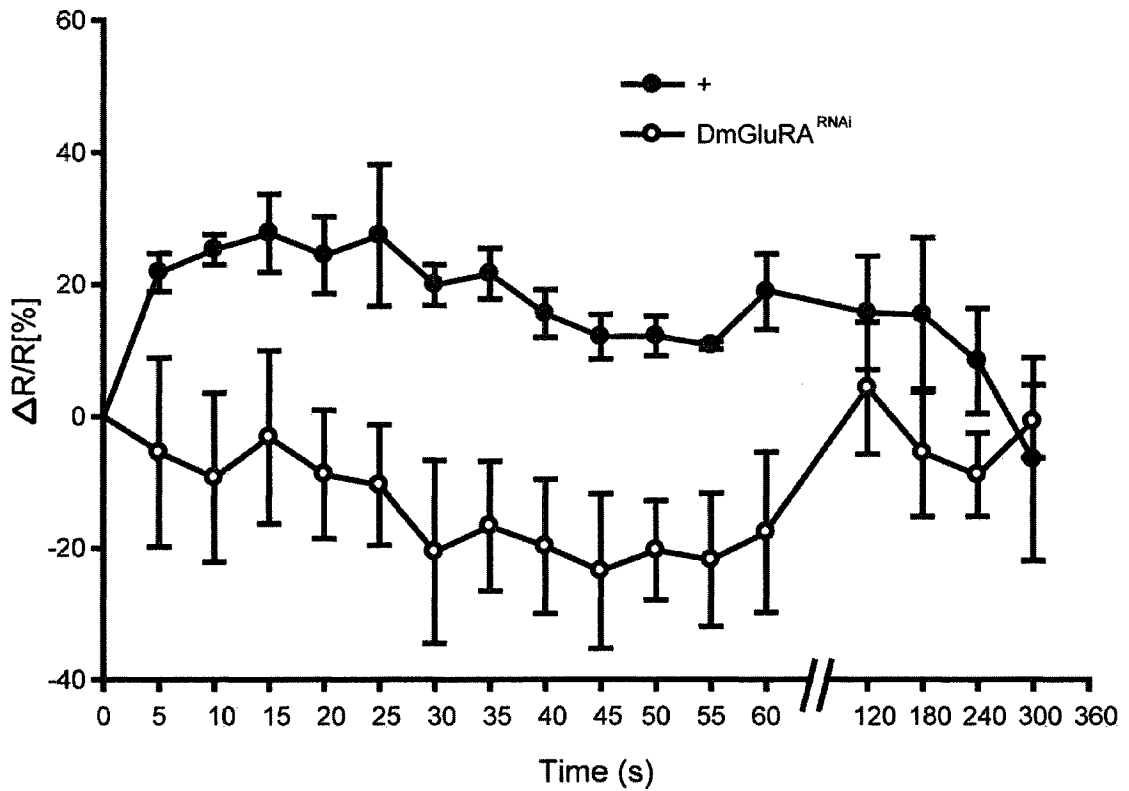
Figure 3.12   Glutamate application stimulates an increase in intracellular Ca^{2+} levels in the DmGluRA$^+$ but not in D42>DmGluRA^{RNAi} mutant larvae nerve terminals. Quantification of FRET signal intensity levels corresponding to levels in *DmGluRA$^+$* and *D42>DmGluRA^{RNAi}* larvae every 5 seconds after an initial 100 µM glutamate application (final bath concentration). After 1 minute, measurements were taken on the minute for four subsequent minutes. Pixel intensities were quantified using ImageJ software and background subtraction was performed as described in detail in Methods section. Circles represent mean normalized synaptic FRET signal intensity levels +/- SEMs. n values from *top* to *bottom* are 8, and 4 respectively.

57

3.10 FAK and Ras are possible mediators of DmGluRA dependant activation of PI3K

Another plausible intermediate between DmGluRA and PI3K activation is the Ras oncogene. In many cell types the PI3K pathway is an effector of the Ras signaling. the Stern lab has already shown that Ras regulates PI3K activity in the peripheral glia (Lavery et al., 2007) and in the prothoracic gland (PG) (Caldwell et al., 2005) so it seems plausible that Ras could activate PI3K in the nerve terminal as well.

If Ras activity leads to the activation of the PI3K pathway, then inhibition of Ras via expression of a dominant negative transgene (Ras^{N17}) is predicted to mimic the hyperexcitability observed when PI3K pathway activity is blocked in motor neurons, whereas hyperactivation of Ras via introduction of null mutations in the Ras-GAP neurofibromin (NF1) is predicted to mimic the hypoexcitability observed when PI3K activity is elevated in motor neurons. To test these predictions, I measured neuronal excitability in larvae overexpressing Ras^{N17} *(Lee et al., 1996)* in motor neurons and in $NF1^{P1}$ null mutant larvae (The et al., 1997). Unfortunately, larvae overexpressing the constitutively active Ras^{v12} transgene were embryonic lethal. I found that overexpression of Ras^{N17}

58
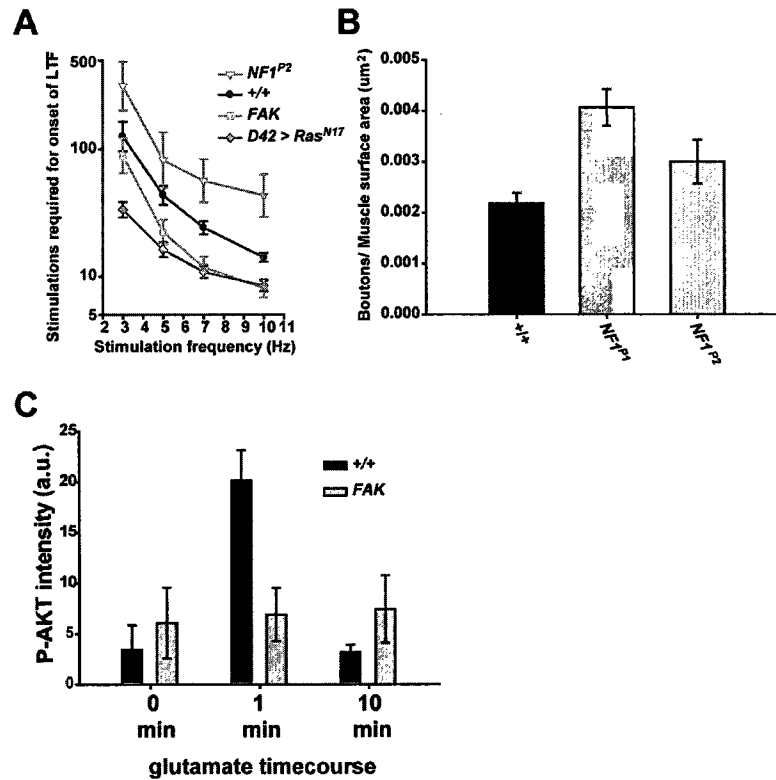
Figure 3.13 Ras and FAK likely mediate the activation of PI3k by DmGluRA.
A, Quantification of the rate of onset of long term facilitation for each genotype. The bath $[Ca^{2+}]$ was 0.15 mM. A 100 μM concentration of quinidine was present in the recording solution. The geometric mean of number of stimulations required for the onset of long-term facilitation at the indicated stimulus frequencies is shown for each genotype. From *top* to *bottom*, n = 4, 15, 6 and 10, respectively, for each genotype. Error bars represent +/-SEMs. B, Mean number (+/- S.E.M.s) of synaptic boutons normalized to the surface area of muscle 6 at abdominal segment A3 in the indicated genotypes. From left to right, n=19, 21, and 18 respectively, for each genotype. Arborization experiment conducted in large part by Alexandra Mirina. C, Quantification of phosphorylated Akt (p-Akt) levels in $DmGluRA^{+}$, and *FAK* mutant larvae immediately prior to glutamate application, after 1 min of 100 μM glutamate application (final bath concentration), and 10 min after a wash with glutamate free media. Nerve terminals were outlined with HRP fluorescence as reference. Pixel intensities were quantified using ImageJ software and background subtraction was performed as described in detail in Methods section. Bars represent mean synaptic p-Akt levels +/- SEMs. The P-AKT experiment was conducted in large part by Elaina Bolinger.

59

increased the rate of onset of LTF to a level very similar to that observed when PI3K pathway activity was decreased whereas in $NF1^{P1}$ null mutant larvae, the rate of onset of LTF was decreased to levels very similar to those observed when *PI3K-CAAX* was expressed in motor neurons (Figure 3.13 A).

If PI3K is an effector of Ras in the nerve terminal, then it is predicted that hyperactivation of Ras should also phenocopy the synaptic growth observed when PI3K is hyperactivated. In order to test this prediction, I measured synaptic arborization in $NF1^{P1}$ and $NF1^{P2}$ null mutant larvae. I found that both $NF1^{P1}$ and $NF1^{P2}$ null mutant larvae exhibit increases in synaptic arborization similar to those observed in larvae overexpressing *D42 > PI3K-CAAX* in motor neurons (Figure 3.13 B).

These data raise the possiblity that Ras is an important regulator of PI3K in motor nerve terminals. However, the observed fold increase in $NF1^{P1}$ and $NF1^{P2}$ null mutant larvae over the wildtype control is not as great as the extent observed in *D42 > PI3K-CAAX* over its *D42 > +* control. For this experiment, an isogenic wildtype stock (s880) was used as the wildtype control instead of the *D42 > +* used in the arborization studies reported above. I found s880 larvae to exhibit bouton densities that were slightly higher than those in the *D42 > +* control larvae. This difference could be due to differences in genetic backgrounds between s880, *Nf1,* and *D42* larvae. Alternatively, the phenotypic discrepancies could reveal that a second activator of PI3K is active at the motor nerve terminal

60

A second candidate regulator of PI3K is the focal adhesion kinase (FAK), which has been shown to activate PI3K directly via the SH3-domain of p85α (Guinebault et al., 1995) and can also increase Ras activity when overexpressed (Schlaepfer and Hunter, 1997). In addition, FAK itself can be activated by increases in intracellular Ca^{2+} (Giannone et al., 2004), making FAK activation of PI3K consistent with the hypothesis explored above.

If FAK is necessary for activation of PI3K in motor nerve terminals, it is predicted that loss of function of FAK via null alleles should phenocopy the inactivation of PI3K activity, either by dominant negative transgene or overexpression of *PTEN*. In order to test this hypothesis I measured the rate of onset of LTF in *FAK* null mutant larvae. As expected, *FAK* mutant larvae exhibit an increase in the rate of onset of LTF consistent with my hypothesis (Figure 3.13 A). While the hyperexcitability observed in *FAK* mutants does raise the possibility that FAK can activate PI3K in motor neurons, the hyperexcitability could be the consequence of an unrelated, non-PI3K mediated effect.

In order to test whether FAK is directly mediating the activation of PI3K activity by DmGluRA, I assayed the P-Akt levels of *FAK* mutant larvae upon application of glutamate, as described above. I found that *FAK* mutant larvae are unable to illicit an increase in P-Akt in response to glutamate (Figure 3.13 C) similar to the phenotype observed for *DmGluRA^{112b}* mutant larvae. This suggests that FAK does indeed mediate the activation of PI3K by DmGluRA.

61

Chapter 4: Discussion

4.1 Synopsis

Here I show that glutamate-mediated activation of DmGluRA decreases neuronal excitability by activating the lipid kinase PI3 kinase (PI3K), which promotes growth and inhibits apoptosis in various cell types. In particular, I report that transgene-induced inhibition of PI3K in motor neurons confers neuronal excitability phenotypes similar to $DmGluRA^{112b}$, whereas transgene-induced activation of PI3K confers the opposite excitability phenotypes. I also show that PI3K activation in motor neurons suppresses the increased excitability of $DmGluRA^{112b}$, and glutamate application to motor nerve terminals activates PI3K in a DmGluRA-dependent manner. Finally, I show that altered PI3K activity regulates both axon diameter and synapse number, and that these effects on neuronal growth are mediated by the Tor/S6 kinase pathway, whereas the effects of PI3K on neuronal excitability are mediated by the transcription factor Foxo. I conclude that negative feedback of Drosophila motor neuron excitability occurs via the glutamate-induced activation of DmGluRA autoreceptors, causing the PI3K-dependent inhibition of Foxo and a consequent decrease in neuronal excitability. A similar negative feedback operating in the mammalian CNS might underlie neuronal disorders involving the group II mGluRs or PI3K.

4.2 A mechanism for the glutamate-induced negative feedback of motor neuron excitability

The effects on neuronal excitability of altered DmGluRA, PI3K, and Foxo activities are consistent with a model in which glutamate released from motor nerve terminals as a consequence of motor neuron activity activates motor neuron PI3K via DmGluRA autoreceptors, which then downregulate neuronal excitability via inhibition of Foxo (Figure 4.1). Foxo, in turn, might regulate excitability via transcription of ion channel subunits or regulators. Although such putative Foxo targets have not been identified, one potential target might be the translational repressor encoded by *pumilio (pum)*: *pum* expression is downregulated by neuronal activity, Pum decreases transcript levels of the sodium channel encoded by *para*, and both *para* overexpression and *pum* mutations increase rate of onset of LTF in a manner similar to that described here (Loughney et al., 1989; Stern et al., 1990; Schweers et al., 2002; Mee et al., 2004)

63
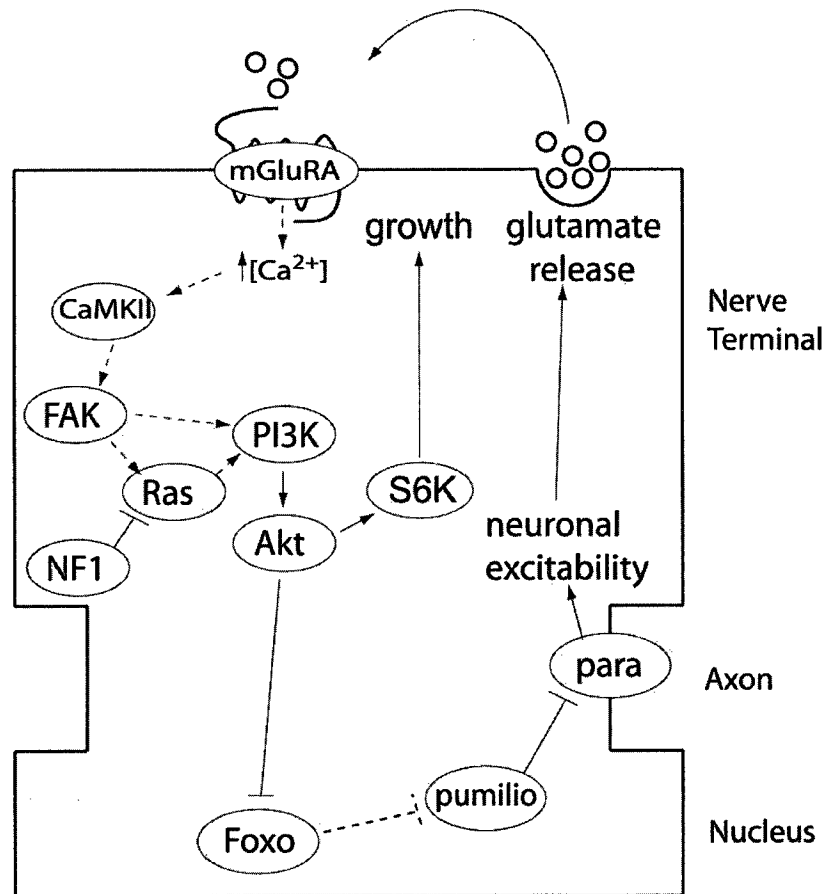
Figure 4.1. A model for the negative feedback loop regulating motor neuron excitability. The transcription factor Foxo increases neuronal excitability through a mechanism possibly involving transcription of ion channel subunits or regulators. This increased excitability promotes glutamate release from motor nerve terminals, which then activates presynaptic DmGluRA in an autocrine manner. This activation, in turn, activates PI3K and the subsequent inactivation of Foxo by Akt-mediated inhibitory phosphorylation. Activated PI3K also promotes axonal growth and synapse formation via the Tor/S6K pathway. Dotted lines represent hypothetical interactions.

64

4.3 Other negative feedback systems at the Drosophila nmj

The DmGluRA-dependent negative feedback reported here co-exists with several other negative feedback systems operating at the Drosophila nmj. In addition to altered excitability, these systems include alterations in the vesicle release properties of the motor nerve terminal and density of the muscle glutamate receptors (Davis, 2006). Presumably, these diverse feedback systems, acting in parallel, regulate specific aspects of neuronal function. The DmGluRA-dependent feedback system reported here differs in several respects from some of the other feedback systems reported. For example, this DmGluRA-dependent feedback apparently involves transcriptional changes, suggesting that this system operates on a long time scale and thus will be responsive to chronic, rather than acute, changes in neuronal activity. In addition, this system is likely to be motor neuron-cell autonomous, and will not involve participation of additional cells, such as target muscles or adjacent glia. Furthermore, this system is predicted to link mechanistically several PI3K-dependent processes, including activity-dependent downregulation of neuronal excitability and upregulation of neuronal growth. In this regard, the PI3K-dependent inhibition of Foxo might protect neurons from excitotoxic effects of prolonged stimulation; such protection would not be accomplished by the other feedback systems operating.

65

4.4 Role of mammalian mGlur's and PI3K in regulation of ion channel activity

Both mGluRs and PI3K have been previously implicated in regulation of ion channel activity. For example, ligand activation of group I mGluRs trigger $G\alpha q$-mediated release of Ca^{2+} from intracellular stores, and consequently activate Ca^{2+}-dependent K^+ channels and nonselective cation channels (Fagni et al., 2000), whereas activation of group II mGluRs inhibit transmitter release via inhibition of P/Q Ca^{2+} channels (Robbe et al., 2002; Mela et al., 2006). PI3K activation can promote ion channel insertion into cell membranes (Dryer et al., 2003; Viard et al., 2004; Hou et al., 2008) and can mediate the decrease in excitability conferred by application of leptin, the product of the obese gene, by activating Ca^{2+}-dependent K^+ channels (Shanley et al., 2002). However, to my knowledge, effects of mGluR or PI3K activation on ion channel transcription in the nervous system have not been reported.

PI3K also regulates ion channel activity in non-excitable cells. PI3K mediates the ability of insulin growth factor to activate the Eag channel, and the ability of serum to activate the intermediate-conductance Ca^{2+}-activated K^+ channel in breast carcinoma and lymphoma cells, respectively (Borowiec et al., 2007; Wang et al., 2007). Interestingly, in these non-excitable cells, activation is accomplished by both acute effects on channel activity as well as long term effects as a consequence of increased channel transcription. Therefore, PI3K

66

can regulate channel activity over different time courses, and via distinct

mechanisms, presumably via distinct effector pathways.

4.5 Neuronal excitability in human disease

Human orthologues of group II mGluRs and PI3K are implicated in several

neurological disorders. For example, group II mGluRs are potential drug targets

for schizophrenia, epilepsy, and anxiety disorders (Swanson et al., 2005;

Alexander and Godwin, 2006; Patil et al., 2007), raising the possibility that

altered excitability of glutamatergic neurons might play a role in these disorders.

In addition, levels of phospho-Foxo, a product of PI3K/Akt activity, are increased

following induction of seizures in rats, and in the hippocampi of epileptic patients

(Shinoda et al., 2004). This activity-induced increase in phospho-Foxo was

interpreted as a mechanism to protect neurons from the excitotoxic effects of

excessive glutamate release because Foxo is more likely than phospho-Foxo to

promote apoptosis. my results raise the possibility that this increase in phospho-

Foxo levels occurs via glutamate-induced PI3K activation mediated by group II

mGluRs, and interpret this increase as a negative feedback on excitability. A role

for PI3K activity in inhibiting epileptic seizures is further supported by the recent

observation that application of leptin, a known PI3K activator, inhibits seizures in

a PI3K-dependent manner (Xu et al., 2008). Increased insulin/IGF levels and

increased PI3K activity are also implicated in autism spectrum disorders (Kwon

67

et al., 2006; Mills et al., 2007). These increases are generally hypothesized to affect neuronal function by increasing arborization and synapse formation, but my results raise the possibility that altered neuronal excitability might also contribute. Thus, the results reported here might have significance for several human neurological disorders.

4.6 A novel signaling pathway linking group II mGluRs and PI3K

The mechanism by which glutamate-activated DmGluRA activates PI3K remains unknown. Although, as discussed above, mammalian group I mGluRs activate PI3K via the Homer scaffolding protein and the PI3K enhancer PIKE (Rong et al., 2003), Drosophila mGluRA, similar to mammalian group II mGluRs, lack Homer binding motifs (Diagana et al., 2002) and thus would not be predicted to activate PI3K by this mechanism. Alternatively, although the inhibition of glutamate-induced p-Akt activation by $PI3K^{DN}$ expression demonstrates that PI3K activity is required for this activation, it remains possible that glutamate increases p-Akt levels by activating an enzyme in addition to PI3K. For example, Akt is reported to be phosphorylated and activated by Calmodulin-dependent kinase kinase (Yano et al., 1998). Additionally, glutamate-activated DmGluRA might activate PI3K in motor nerve terminals indirectly by triggering Ca^{2+} release from stores, leading to release of insulin and hence activation of PI3K by well-

established mechanisms. Further experiments will be required to address these issues.

4.7 Future Work

4.7.1   Determine the mechanism by which DmGluRA activates PI3K in the nerve terminal

Calcium signaling

As described above, intracellular Ca^{2+} signaling is an attractive candidate for an intermediary between DmGluRA and PI3K. It is known that group II mGluRs can initiate elevation of intracellular Ca^{2+} and there are several mechanisms by which Ca^{2+} signaling can lead to the activation of PI3K.

While the data presented above demonstrate that glutamate application to the nerve terminal can induce elevation of Ca^{2+} levels within the nerve terminal, and that this is DmGluRA dependent, the methodology used can be improved upon to gain a more detailed picture of the dynamics of the Ca^{2+} transient initiated by DmGluRA activity. The Cameleon 2.1 transgene has several drawbacks that limit its usefulness by the Stern lab. The foremost of these drawbacks is purely technical, yet limiting nonetheless. For optimal measurement, the use of a FRET based Ca^{2+} indicator requires a scope and camera system that allows for two simultaneous images to be taken: one in the 535 nm spectrum and another in the 485 spectrum. The fluorescence scope that I have access to does not have the

69

capability of taking two images simultaneously. Despite taking the images as quickly as possible, the mechanics of the scope do not allow for the proper filter cubes to be set in place in less than a second. This causes a delay between the capturing of the two images, which in turn could skew the data. While there are other scopes available with the capability of capturing two simultaneous images at different wavelengths, they are inverted scopes and thus are unsuitable to the Stern lab dissection technique which requires a larva placed upright, pinned in an open dissection tray.

The above mentioned problem can be avoided, however, by the use of a single fluorophore genetically encoded calcium indicator (GECI) such as the *camgaroo* or *GCaMP* 3.1 GECIs. These transgenic indicators employ circularly permutated fluorophores in which the interaction of Ca^{2+} with CaM induce a conformational change within the fluorophore that increases its fluorescence (Kotlikoff, 2007). With the use of these single fluorophores based indicators, only a single image would need to be taken. This would also aid a great deal in post collection data analysis.

Steps should also be taken to attempt to quantitate the amount of Ca^{2+} present within the nerve terminals. This can be accomplished by calibrating each sample with a maximum, via application of Ca^{2+} ionophores, and minimum via EGTA induced Ca^{2+} chelation (Palmer and Tsien, 2006).

These technical details aside, assaying for the presence or absence of a Ca^{2+} transient upon glutamate application has great potential in helping to dissect which molecules are responsible for the activation of PI3K by DmGluRA. Two

70

important questions remain unanswered regarding the Ca^{2+} transient described in figure 3.12: Is the source of this Ca^{2+} from outside the cell, or from internal stores, and if it is from internal stores, is the Ca^{2+} release mediated by the ryanodine receptor or the IP3R? If the Ca^{2+} transient is from IP3R mediated release from internal stores, then inhibition of the IP3R with an RNAi transgene should inhibit the glutamate induced Ca^{2+} increase.

4.7.2   Determine the transcriptional target of Foxo that is regulating neuronal excitability

Another important unanswered question is what is the transcriptional target of Foxo that regulates neuronal excitability. As discussed above, a very attractive candidate is the translational repressor pumilio which has been shown to regulate the sodium channel Para (Mee et al., 2004). If Foxo does indeed inhibit pum, I predict that in flies carrying the $Foxo^{21}/Foxo^{25}$ null combination, protein levels of pumilio should be elevated. This experiment has recently been performed by Curtis Lin in the Stern lab, and preliminary data suggest that pum levels are increased as predicted in $Foxo^{21}/Foxo^{25}$ null flies. Levels of pum could also be tested immunohistochemically to determine if they are increased at the nerve terminal as compared to wildtype, and *pum* transcript levels could be tested using Q-PCR methods. While these experiments would strongly suggest that Foxo led to the transcriptional inhibition of pum, it would not necessarily be indicative of a direct inhibition of

71

pum by Foxo. It is entirely plausible to think that Foxo itself regulates the transcription of a second unidentified gene that in turn inhibits pum.

72

Chapter 5: The effects of larval nutrition on neuronal excitability and nmj growth

5.1 Introduction

While investigating the role of PI3K in regulating motor neuron excitability, I observed that larvae deficient for PI3K (heteroallelic combination of a loss of function mutation $PI3K^A$ and a hypomorphic mutation $PI3K^{2H1}$) exhibited a marked decrease in neuronal excitability as measured by the rate of onset of LTF (Figure 5.1 A). This observation seems contradictory to the evidence reported in the previous chapter showing that motor neuron specific decreases in PI3K activity lead to an increase in neuronal excitability (Figure 3.2). A possible explanation of this contradiction is that PI3K activity can regulate neuronal excitability in a cell non-autonomous manner. For example, PI3K levels in another tissue such could regulate the production or release of a growth factor or other signaling molecule which in turn acts on the motor neuron to regulate excitability. In addition to alterations in neuronal excitability, *PI3K* deficient larvae were developmentally delayed, reaching third instar larval stage both late and at a much smaller size than their wildtype counterparts. Interestingly, small size, developmental delay, and decreased neuronal excitability can also be observed in larvae whose diets have been calorically restricted, either by nutritionally deficient food (reviewed in Pletcher et al., 2005) or larvae found in older,

73

overcrowded bottles where food is less plentiful (unpublished Stern lab observations). Caloric restriction is well documented in mammals as a means of reducing neuronal excitability and has even been used as a treatment for epilepsy (Bough and Rho, 2007), however little is known about the molecular mechanisms behind this phenomenon. As such, my data raise the possibility that PI3K could play an integral role in the nutrition dependent regulation of neuronal excitability.

5.2 Results

5.2.1 Global larval insulin levels affect the excitability of Drosophila motor axons and growth at the nerve terminal

Since the Drosophila insulin receptor signals via the PI3K pathway (reviewed in Johnston et al., 2003), and insulin levels are directly dependent upon caloric intake, I hypothesize that ablation of the insulin producing cells (IPCs) that produce three Drosophila insulin homologues, the Drosophila insulin like peptides 2, 3, and 5 (dilp2, dilp3, and dilp5 respectively) in the Drosophila brain, should phenocopy both a restricted diet and a loss of function of PI3K. When I ablated these neurons using *dilp2Gal4* to drive expression of the apoptosis inducing *reaper (rpr)* gene I in fact did observe both a decrease in

74

neuronal excitability and a marked developmental delay (Figure 5.1 A, and data not shown), supporting my hypothesis.

To test whether PI3K was required within the insulin producing cells (IPCs) directly, I decreased PI3K activity specifically in these neurons using the $PI3K^{DN}$ transgene, but observed only a modest decrease in excitability as compared to wildtype (Figure 5.1 A). Suprisingly, however, increasing PI3K activity in these neurons by overexpression of PI3K-CAAX induced a significant increase in excitability (Figure 5.1 A).

Our hypothesis also predicts that an increase in insulin levels should produce larvae who exhibit an increase in neuronal excitability. Magdalena Walkiewicz in the Stern lab has previously shown that expression of a constitutively active PKA transgene ($PKAR^*$) within the IPCs leads to an increase in larval insulin levels. I observed that larvae overexpressing $PKAR^*$ within the IPCs also exhibited a decrease in rate of onset of LTF (Figure 5.1 A), contrary to my prediction. One could envision a different model, however, that could explain this result. In this model, if insulin levels are low, due to caloric restriction or ablation of the insulin producing cells, a cell non-autonomous pathway regulates neuronal excitability, perhaps via the peripheral glia. However, when insulin levels are high, for instance either under conditions of increased food consumption or transgenic overexpression of $PKAR^*$ within the IPCs, insulin acts directly on the motor neuron, activating the PI3K pathway via the Insulin receptor. In this view, activation of PI3K within the motor neuron would decrease motor neuron excitability via inhibition of Foxo as described in Chapter 3.
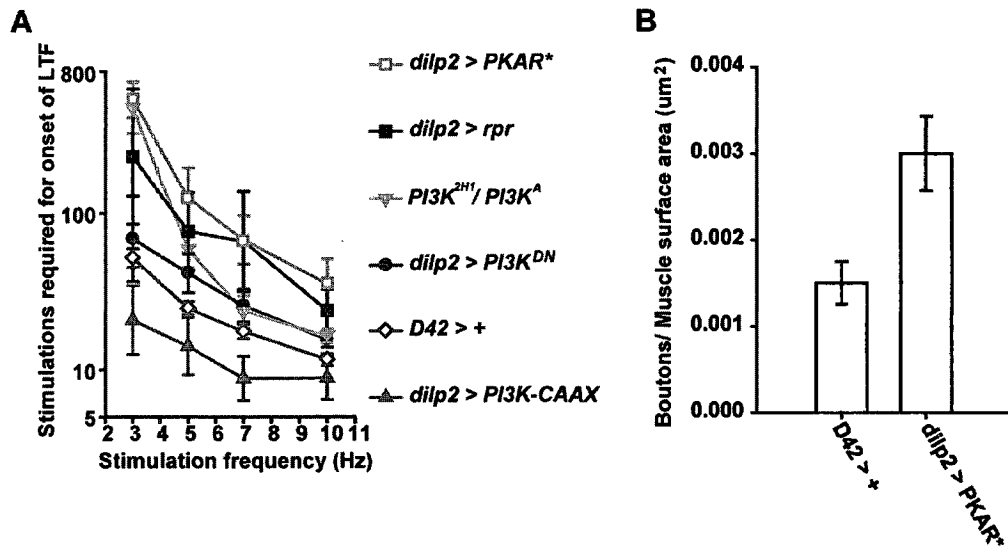
75

Figure 5.1. Insulin released from the insulin producing cells (IPC's) in the CNS modulate neuronal excitability and synapse formation. A) Quantification of the rate of onset of long term facilitation for each genotype. The bath $[Ca^{2+}]$ was 0.15 mM. A 100 μM concentration of quinidine was present in the recording solution. The geometric mean of number of stimulations required for the onset of long-term facilitation at the indicated stimulus frequencies is shown for each genotype. Error bars represent SEMs. B, Mean number (+/- S.E.M.s) of synaptic boutons normalized to the surface area of muscle 6 at abdominal segment A3 in the indicated genotypes. From left to right, n=6 and 18 respectively, for each genotype. Arborization experiment conducted in large part by Alexandra Mirina

76

If insulin is activating PI3K in the nerve terminal, then it is predicted that increasing larval insulin levels should phenocopy the synaptic growth observed when PI3K is hyperactivated. In order to test this prediction, I measured synaptic arborization in larvae overexpressing $PKAR^*$ in the IPCs. I found that $dilp2 > PKAR^{2+}$ larvae exhibit increases in synaptic arborization as is predicted by my model (Figure 5.1 B).

5.2.2   Adipokinetic horomone (Akh) levels affect both neuronal excitability and growth at the neuromuscular junction

In order to explain the dichotomy in results described above, I examined the role of PI3K in the corpus cardiacum (CC) which produces the Drosophila analog of glucagon, adipokinetic hormone (AKH). First, I observed that ablation of the CC using $AKHGal4$ to drive expression of rpr resulted in hypoexcitable larvae (Figure 5.2), suggesting that AKH, as well as insulin, positively regulates neuronal excitability. When I altered PI3K activity in the CC, either by increasing its activity by overexpression of $PI3K$-$CAAX$ or decreasing its activity by expression of $PI3K^{DN}$, I observed larvae that were hyperexcitable and hypoexcitable respectively (Figure 5.2). In addition, overexpression of Akh in the
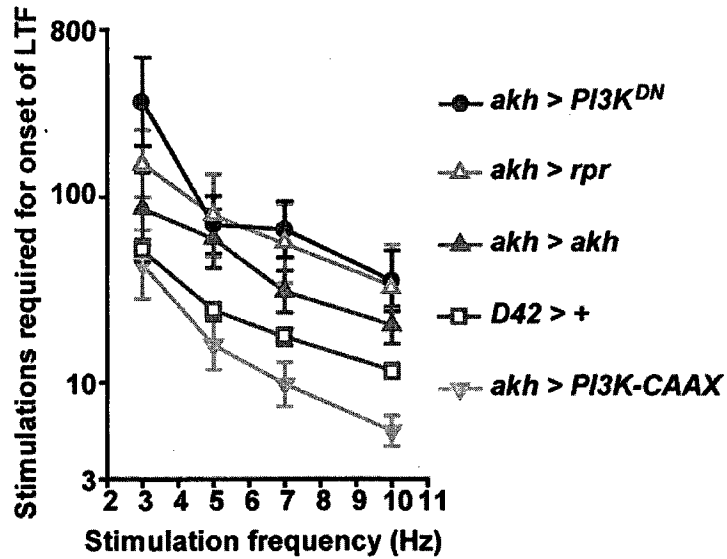
Figure 5.2. Adipokinetic hormone (Akh) regulates neuronal excitability.
Quantification of the rate of onset of long term facilitation for each genotype. The
bath $[Ca^{2+}]$ was 0.15 mM. A 100 µM concentration of quinidine was present in the
recording solution. The geometric mean of number of stimulations required for the
onset of long-term facilitation at the indicated stimulus frequencies is shown for
each genotype. From *top* to *bottom*, n = 5, 6, 6, 18, and 6, respectively, for each
genotype. Error bars represent +/- SEMs.

78

CC itself lead to an increase in excitability, similar to when PI3K activity is increased in the CC. Since the dilp2 producing neurons are positioned adjacent to the CC and have been suggested to release dilp2 directly onto the CC (Rulifson et al., 2002), this suggests that Akh production is dependent upon PI3K activity, and that AKH levels have a positive effect on neuronal excitability.

5.3 Discussion

Further work is required to further elucidate the mechanisms behind the nutritional relation to neuronal excitability. One question that remains is through which tissue AKH is acting to modulate neuronal excitability. While it is tempting to suggest that AKH and the dilps act directly on the motor neuron itself, it is unclear as to how these hormones could reach the motor neuron, since there is no direct contact between the motor neurons and the haemolymph. An attractive candidate is the peripheral glia, which forms the blood brain barrier, its well characterized communication with the motor neuron (reviewed in Lemke, 2001), and its suspected role in modulating neuronal excitability. In order to examine which tissue is modulating neuronal excitability, however, first I must document the relationship between nutrition and neuronal excitability. To accomplish this I plan to measure the electrophysiological properties of larvae raised on food of

79

varying nutritional content. Once this is established, I plan to express AKH in the peripheral glia of starved larvae. If my hypothesis is correct, this should rescue the decrease in excitability observed in calorically restricted larvae. Secondly, expression of an AKH^{RNAi} transgene in the peripheral glia of wildtype larvae should phenocopy calorically restricted larvae. If these experiments yield the expected results, further explorations will include epistasis tests to determine through which signaling pathway AKH is signaling with the peripheral glia.

Chapter 6: Referenced Works

Aiba A, Kano M, Chen C, Stanton ME, Fox GD, Herrup K, Zwingman TA, Tonegawa S (1994) Deficient cerebellar long-term depression and impaired motor learning in mGluR1 mutant mice. Cell 79:377-388.

Alexander GM, Godwin DW (2006) Metabotropic glutamate receptors as a strategic target for the treatment of epilepsy. Epilepsy Res 71:1-22.

Allen MJ, Shan X, Caruccio P, Froggett SJ, Moffat KG, Murphey RK (1999) Targeted expression of truncated glued disrupts giant fiber synapse formation in Drosophila. J Neurosci 19:9374-9384.

Anwyl R (1999) Metabotropic glutamate receptors: electrophysiological properties and role in plasticity. Brain Res Brain Res Rev 29:83-120.

Barcelo H, Stewart MJ (2002) Altering Drosophila S6 kinase activity is consistent with a role for S6 kinase in growth. Genesis 34:83-85.

Bashir ZI, Jane DE, Sunter DC, Watkins JC, Collingridge GL (1993) Metabotropic glutamate receptors contribute to the induction of long-term depression in the CA1 region of the hippocampus. Eur J Pharmacol 239:265-266.

Bogdanik L, Mohrmann R, Ramaekers A, Bockaert J, Grau Y, Broadie K, Parmentier ML (2004) The Drosophila metabotropic glutamate receptor DmGluRA regulates activity-dependent synaptic facilitation and fine synaptic morphology. J Neurosci 24:9105-9116.

Borowiec AS, Hague F, Harir N, Guenin S, Guerineau F, Gouilleux F, Roudbaraki M, Lassoued K, Ouadid-Ahidouch H (2007) IGF-1 activates hEAG K(+) channels through an Akt-dependent signaling pathway in breast cancer cells: role in cell proliferation. J Cell Physiol 212:690-701.

Bortolotto ZA, Collingridge GL (1993) Characterisation of LTP induced by the activation of glutamate metabotropic receptors in area CA1 of the hippocampus. Neuropharmacology 32:1-9.

Bough KJ, Rho JM (2007) Anticonvulsant mechanisms of the ketogenic diet. Epilepsia 48:43-58.

Brand AH, Perrimon N (1993) Targeted gene expression as a means of altering cell fates and generating dominant phenotypes. Development 118:401-415.

Broughton SJ, Kitamoto T, Greenspan RJ (2004) Excitatory and inhibitory switches for courtship in the brain of Drosophila melanogaster. Curr Biol 14:538-547.

Budnik V, Zhong Y, Wu CF (1990) Morphological plasticity of motor axons in Drosophila mutants with altered excitability. J Neurosci 10:3754-3768.

Caldwell PE, Walkiewicz M, Stern M (2005) Ras activity in the Drosophila prothoracic gland regulates body size and developmental rate via ecdysone release. Curr Biol 15:1785-1795.

Catania MV, Bellomo M, Di Giorgi-Gerevini V, Seminara G, Giuffrida R, Romeo R, De Blasi A, Nicoletti F (2001) Endogenous activation of group-I

metabotropic glutamate receptors is required for differentiation and survival of cerebellar Purkinje cells. J Neurosci 21:7664-7673.

Chen CY, Ling Eh EH, Horowitz JM, Bonham AC (2002) Synaptic transmission in nucleus tractus solitarius is depressed by Group II and III but not Group I presynaptic metabotropic glutamate receptors in rats. J Physiol 538:773-786.

Choe CU, Ehrlich BE (2006) The inositol 1,4,5-trisphosphate receptor (IP3R) and its regulators: sometimes good and sometimes bad teamwork. Sci STKE 2006:re15.

Chouinard SW, Wilson GF, Schlimgen AK, Ganetzky B (1995) A potassium channel beta subunit related to the aldo-keto reductase superfamily is encoded by the Drosophila hyperkinetic locus. Proc Natl Acad Sci U S A 92:6763-6767.

Colombani J, Bianchini L, Layalle S, Pondeville E, Dauphin-Villemant C, Antoniewski C, Carre C, Noselli S, Leopold P (2005) Antagonistic actions of ecdysone and insulins determine final size in Drosophila. Science 310:667-670.

Cross DA, Alessi DR, Cohen P, Andjelkovich M, Hemmings BA (1995) Inhibition of glycogen synthase kinase-3 by insulin mediated by protein kinase B. Nature 378:785-789.

Davis GW (2006) Homeostatic Control of Neural Activity: From Phenomenology to Molecular Design. Annu Rev Neurosci.

Davis GW, Schuster CM, Goodman CS (1996) Genetic dissection of structural and functional components of synaptic plasticity. III. CREB is necessary for presynaptic functional plasticity. Neuron 17:669-679.

Desai NS, Rutherford LC, Turrigiano GG (1999) Plasticity in the intrinsic excitability of cortical pyramidal neurons. Nat Neurosci 2:515-520.

Diagana TT, Thomas U, Prokopenko SN, Xiao B, Worley PF, Thomas JB (2002) Mutation of Drosophila homer disrupts control of locomotor activity and behavioral plasticity. J Neurosci 22:428-436.

Dionne MS, Pham LN, Shirasu-Hiza M, Schneider DS (2006) Akt and FOXO dysregulation contribute to infection-induced wasting in Drosophila. Curr Biol 16:1977-1985.

Dryer SE, Lhuillier L, Cameron JS, Martin-Caraballo M (2003) Expression of K(Ca) channels in identified populations of developing vertebrate neurons: role of neurotrophic factors and activity. J Physiol Paris 97:49-58.

Duffy JB (2002) GAL4 system in Drosophila: a fly geneticist's Swiss army knife. Genesis 34:1-15.

Eaton BA, Fetter RD, Davis GW (2002) Dynactin is necessary for synapse stabilization. Neuron 34:729-741.

Echegoyen J, Neu A, Graber KD, Soltesz I (2007) Homeostatic plasticity studied using in vivo hippocampal activity-blockade: synaptic scaling, intrinsic plasticity and age-dependence. PLoS ONE 2:e700.

Enz R (2007) The trick of the tail: protein-protein interactions of metabotropic glutamate receptors. Bioessays 29:60-73.

Fagni L, Chavis P, Ango F, Bockaert J (2000) Complex interactions between mGluRs, intracellular Ca2+ stores and ion channels in neurons. Trends Neurosci 23:80-88.

Ferraguti F, Shigemoto R (2006) Metabotropic glutamate receptors. Cell Tissue Res 326:483-504.

Fiorillo CD, Williams JT (1998) Glutamate mediates an inhibitory postsynaptic potential in dopamine neurons. Nature 394:78-82.

Ganetzky B, Wu CF (1982) Drosophila mutants with opposing effects on nerve excitability: genetic and spatial interactions in repetitive firing. J Neurophysiol 47:501-514.

Giannone G, Ronde P, Gaire M, Beaudouin J, Haiech J, Ellenberg J, Takeda K (2004) Calcium rises locally trigger focal adhesion disassembly and enhance residency of focal adhesion kinase at focal adhesions. J Biol Chem 279:28715-28723.

Gibson JR, Bartley AF, Huber KM (2006) Role for the subthreshold currents ILeak and IH in the homeostatic control of excitability in neocortical somatostatin-positive inhibitory neurons. J Neurophysiol 96:420-432.

Glaum SR, Miller RJ (1992) Metabotropic glutamate receptors mediate excitatory transmission in the nucleus of the solitary tract. J Neurosci 12:2251-2258.

Gorczyca M, Augart C, Budnik V (1993) Insulin-like receptor and insulin-like peptide are localized at neuromuscular junctions in Drosophila. J Neurosci 13:3692-3704.

Greenspan RJ (1997) Fly pushing : the theory and practice of Drosophila genetics. Plainview, N.Y.: Cold Spring Harbor Laboratory Press.

Guinebault C, Payrastre B, Racaud-Sultan C, Mazarguil H, Breton M, Mauco G, Plantavid M, Chap H (1995) Integrin-dependent translocation of phosphoinositide 3-kinase to the cytoskeleton of thrombin-activated platelets involves specific interactions of p85 alpha with actin filaments and focal adhesion kinase. J Cell Biol 129:831-842.

Hay N, Sonenberg N (2004) Upstream and downstream of mTOR. Genes Dev 18:1926-1945.

Hou Q, Zhang D, Jarzylo L, Huganir RL, Man HY (2008) Homeostatic regulation of AMPA receptor expression at single hippocampal synapses. Proc Natl Acad Sci U S A 105:775-780.

Houamed KM, Kuijper JL, Gilbert TL, Haldeman BA, O'Hara PJ, Mulvihill ER, Almers W, Hagen FS (1991) Cloning, expression, and gene structure of a G protein-coupled glutamate receptor from rat brain. Science 252:1318-1321.

Huang Y, Stern M (2002) In vivo properties of the Drosophila inebriated-encoded neurotransmitter transporter. J Neurosci 22:1698-1708.

Hwangbo DS, Gershman B, Tu MP, Palmer M, Tatar M (2004) Drosophila
dFOXO controls lifespan and regulates insulin signalling in brain and fat
body. Nature 429:562-566.

Jan YN, Jan LY (1978) Genetic dissection of short-term and long-term facilitation
at the Drosophila neuromuscular junction. Proc Natl Acad Sci U S A
75:515-519.

Jo J, Heon S, Kim MJ, Son GH, Park Y, Henley JM, Weiss JL, Sheng M,
Collingridge GL, Cho K (2008) Metabotropic glutamate receptor-mediated
LTD involves two interacting Ca(2+) sensors, NCS-1 and PICK1. Neuron
60:1095-1111.

Johnston AM, Pirola L, Van Obberghen E (2003) Molecular mechanisms of
insulin receptor substrate protein-mediated modulation of insulin
signalling. FEBS Lett 546:32-36.

Junger MA, Rintelen F, Stocker H, Wasserman JD, Vegh M, Radimerski T,
Greenberg ME, Hafen E (2003) The Drosophila forkhead transcription
factor FOXO mediates the reduction in cell number associated with
reduced insulin signaling. J Biol 2:20.

Kew JN, Ducarre JM, Pflimlin MC, Mutel V, Kemp JA (2001) Activity-dependent
presynaptic autoinhibition by group II metabotropic glutamate receptors at
the perforant path inputs to the dentate gyrus and CA1.
Neuropharmacology 40:20-27.

Knox S, Ge H, Dimitroff BD, Ren Y, Howe KA, Arsham AM, Easterday MC,
Neufeld TP, O'Connor MB, Selleck SB (2007) Mechanisms of TSC-

mediated control of synapse assembly and axon guidance. PLoS ONE 2:e375.

Kotlikoff MI (2007) Genetically encoded Ca2+ indicators: using genetics and molecular design to understand complex physiology. J Physiol 578:55-67.

Kwon CH, Luikart BW, Powell CM, Zhou J, Matheny SA, Zhang W, Li Y, Baker SJ, Parada LF (2006) Pten regulates neuronal arborization and social interaction in mice. Neuron 50:377-388.

Lavery W, Hall V, Yager JC, Rottgers A, Wells MC, Stern M (2007) Phosphatidylinositol 3-kinase and Akt nonautonomously promote perineurial glial growth in Drosophila peripheral nerves. J Neurosci 27:279-288.

Lee T, Feig L, Montell DJ (1996) Two distinct roles for Ras in a developmentally regulated cell migration. Development 122:409-418.

Leevers SJ, Weinkove D, MacDougall LK, Hafen E, Waterfield MD (1996) The Drosophila phosphoinositide 3-kinase Dp110 promotes cell growth. Embo J 15:6584-6594.

Lemke G (2001) Glial control of neuronal development. Annu Rev Neurosci 24:87-105.

Linden DJ, Connor JA (1992) Long-term Depression of Glutamate Currents in Cultured Cerebellar Purkinje Neurons Does Not Require Nitric Oxide Signalling. Eur J Neurosci 4:10-15.

Loughney K, Kreber R, Ganetzky B (1989) Molecular analysis of the para locus, a sodium channel gene in Drosophila. Cell 58:1143-1154.

Lynch G, Larson J, Kelso S, Barrionuevo G, Schottler F (1983) Intracellular injections of EGTA block induction of hippocampal long-term potentiation. Nature 305:719-721.

Mallart A, Angaut-Petit D, Bourret-Poulain C, Ferrus A (1991) Nerve terminal excitability and neuromuscular transmission in T(X;Y)V7 and Shaker mutants of Drosophila melanogaster. J Neurogenet 7:75-84.

Marder E, Prinz AA (2003) Current compensation in neuronal homeostasis. Neuron 37:2-4.

Martin-Pena A, Acebes A, Rodriguez JR, Sorribes A, de Polavieja GG, Fernandez-Funez P, Ferrus A (2006) Age-independent synaptogenesis by phosphoinositide 3 kinase. J Neurosci 26:10199-10208.

Masu M, Tanabe Y, Tsuchida K, Shigemoto R, Nakanishi S (1991) Sequence and expression of a metabotropic glutamate receptor. Nature 349:760-765.

Mee CJ, Pym EC, Moffat KG, Baines RA (2004) Regulation of neuronal excitability through pumilio-dependent control of a sodium channel gene. J Neurosci 24:8695-8703.

Mela F, Marti M, Fiorentini C, Missale C, Morari M (2006) Group-II metabotropic glutamate receptors negatively modulate NMDA transmission at striatal

cholinergic terminals: role of P/Q-type high voltage activated Ca++ channels and endogenous dopamine. Mol Cell Neurosci 31:284-292.

Mills JL, Hediger ML, Molloy CA, Chrousos GP, Manning-Courtney P, Yu KF, Brasington M, England LJ (2007) Elevated levels of growth-related hormones in autism and autism spectrum disorder. Clin Endocrinol (Oxf) 67:230-237.

Morales-Mulia S, Scholey JM (2005) Spindle pole organization in Drosophila S2 cells by dynein, abnormal spindle protein (Asp), and KLP10A. Mol Biol Cell 16:3176-3186.

Mosca TJ, Carrillo RA, White BH, Keshishian H (2005) Dissection of synaptic excitability phenotypes by using a dominant-negative Shaker K+ channel subunit. Proc Natl Acad Sci U S A 102:3477-3482.

O'Hara PJ, Sheppard PO, Thogersen H, Venezia D, Haldeman BA, McGrane V, Houamed KM, Thomsen C, Gilbert TL, Mulvihill ER (1993) The ligand-binding domain in metabotropic glutamate receptors is related to bacterial periplasmic binding proteins. Neuron 11:41-52.

Palmer AE, Tsien RY (2006) Measuring calcium signaling using genetically targetable fluorescent indicators. Nat Protoc 1:1057-1065.

Palomero T, Sulis ML, Cortina M, Real PJ, Barnes K, Ciofani M, Caparros E, Buteau J, Brown K, Perkins SL, Bhagat G, Agarwal AM, Basso G, Castillo M, Nagase S, Cordon-Cardo C, Parsons R, Zuniga-Pflucker JC, Dominguez M, Ferrando AA (2007) Mutational loss of PTEN induces

90

resistance to NOTCH1 inhibition in T-cell leukemia. Nat Med 13:1203-1210.

Panayotou G (1998) Multiple roles for phosphoinositide 3-kinases in signal transduction. In: Signal Transduction (Heldin C, and Purton, M., ed). Cheltenham: Nelson Thornes.

Parkes TL, Elia AJ, Dickinson D, Hilliker AJ, Phillips JP, Boulianne GL (1998) Extension of Drosophila lifespan by overexpression of human SOD1 in motorneurons. Nat Genet 19:171-174.

Patil ST, Zhang L, Martenyi F, Lowe SL, Jackson KA, Andreev BV, Avedisova AS, Bardenstein LM, Gurovich IY, Morozova MA, Mosolov SN, Neznanov NG, Reznik AM, Smulevich AB, Tochilov VA, Johnson BG, Monn JA, Schoepp DD (2007) Activation of mGlu2/3 receptors as a new approach to treat schizophrenia: a randomized Phase 2 clinical trial. Nat Med 13:1102-1107.

Pin JP, Joly C, Heinemann SF, Bockaert J (1994) Domains involved in the specificity of G protein activation in phospholipase C-coupled metabotropic glutamate receptors. Embo J 13:342-348.

Pletcher SD, Libert S, Skorupa D (2005) Flies and their golden apples: the effect of dietary restriction on Drosophila aging and age-dependent gene expression. Ageing Res Rev 4:451-480.

Poisik O, Raju DV, Verreault M, Rodriguez A, Abeniyi OA, Conn PJ, Smith Y (2005) Metabotropic glutamate receptor 2 modulates excitatory synaptic

transmission in the rat globus pallidus. Neuropharmacology 49 Suppl 1:57-69.

Pozzi D, Condliffe S, Bozzi Y, Chikhladze M, Grumelli C, Proux-Gillardeaux V, Takahashi M, Franceschetti S, Verderio C, Matteoli M (2008) Activity-dependent phosphorylation of Ser187 is required for SNAP-25-negative modulation of neuronal voltage-gated calcium channels. Proc Natl Acad Sci U S A 105:323-328.

Robbe D, Bockaert J, Manzoni OJ (2002) Metabotropic glutamate receptor 2/3-dependent long-term depression in the nucleus accumbens is blocked in morphine withdrawn mice. Eur J Neurosci 16:2231-2235.

Rong R, Ahn JY, Huang H, Nagata E, Kalman D, Kapp JA, Tu J, Worley PF, Snyder SH, Ye K (2003) PI3 kinase enhancer-Homer complex couples mGluRI to PI3 kinase, preventing neuronal apoptosis. Nat Neurosci 6:1153-1161.

Rulifson EJ, Kim SK, Nusse R (2002) Ablation of insulin-producing neurons in flies: growth and diabetic phenotypes. Science 296:1118-1120.

Scanziani M, Salin PA, Vogt KE, Malenka RC, Nicoll RA (1997) Use-dependent increases in glutamate concentration activate presynaptic metabotropic glutamate receptors. Nature 385:630-634.

Schlaepfer DD, Hunter T (1997) Focal adhesion kinase overexpression enhances ras-dependent integrin signaling to ERK2/mitogen-activated protein kinase through interactions with and activation of c-Src. J Biol Chem 272:13189-13195.

Schoepp DD (2001) Unveiling the functions of presynaptic metabotropic
glutamate receptors in the central nervous system. J Pharmacol Exp Ther
299:12-20.

Schoepp DD, Jane DE, Monn JA (1999) Pharmacological agents acting at
subtypes of metabotropic glutamate receptors. Neuropharmacology
38:1431-1476.

Schweers BA, Walters KJ, Stern M (2002) The Drosophila melanogaster
translational repressor pumilio regulates neuronal excitability. Genetics
161:1177-1185.

Sepp KJ, Schulte J, Auld VJ (2000) Developmental dynamics of peripheral glia in
Drosophila melanogaster. Glia 30:122-133.

Shanley LJ, O'Malley D, Irving AJ, Ashford ML, Harvey J (2002) Leptin inhibits
epileptiform-like activity in rat hippocampal neurones via PI 3-kinase-
driven activation of BK channels. J Physiol 545:933-944.

Shinoda S, Schindler CK, Meller R, So NK, Araki T, Yamamoto A, Lan JQ, Taki
W, Simon RP, Henshall DC (2004) Bim regulation may determine
hippocampal vulnerability after injurious seizures and in temporal lobe
epilepsy. J Clin Invest 113:1059-1068.

Sladeczek F, Pin JP, Recasens M, Bockaert J, Weiss S (1985) Glutamate
stimulates inositol phosphate formation in striatal neurones. Nature
317:717-719.

Stern M, Ganetzky B (1989) Altered synaptic transmission in Drosophila hyperkinetic mutants. J Neurogenet 5:215-228.

Stern M, Kreber R, Ganetzky B (1990) Dosage effects of a Drosophila sodium channel gene on behavior and axonal excitability. Genetics 124:133-143.

Stork T, Engelen D, Krudewig A, Silies M, Bainton RJ, Klambt C (2008) Organization and function of the blood-brain barrier in Drosophila. J Neurosci 28:587-597.

Sugiyama H, Ito I, Hirono C (1987) A new type of glutamate receptor linked to inositol phospholipid metabolism. Nature 325:531-533.

Swanson CJ, Bures M, Johnson MP, Linden AM, Monn JA, Schoepp DD (2005) Metabotropic glutamate receptors as novel targets for anxiety and stress disorders. Nat Rev Drug Discov 4:131-144.

Tang ED, Nunez G, Barr FG, Guan KL (1999) Negative regulation of the forkhead transcription factor FKHR by Akt. J Biol Chem 274:16741-16746.

The I, Hannigan GE, Cowley GS, Reginald S, Zhong Y, Gusella JF, Hariharan IK, Bernards A (1997) Rescue of a Drosophila NF1 mutant phenotype by protein kinase A. Science 276:791-794.

Vendra G, Hamilton RS, Davis I (2007) Dynactin suppresses the retrograde movement of apically localized mRNA in Drosophila blastoderm embryos. Rna 13:1860-1867.

Viard P, Butcher AJ, Halet G, Davies A, Nurnberg B, Heblich F, Dolphin AC (2004) PI3K promotes voltage-dependent calcium channel trafficking to the plasma membrane. Nat Neurosci 7:939-946.

Vicario-Abejon C, Owens D, McKay R, Segal M (2002) Role of neurotrophins in central synapse formation and stabilization. Nat Rev Neurosci 3:965-974.

Wang J, Xu YQ, Liang YY, Gongora R, Warnock DG, Ma HP (2007) An intermediate-conductance Ca(2+)-activated K (+) channel mediates B lymphoma cell cycle progression induced by serum. Pflugers Arch 454:945-956.

Watkins JC, Evans RH (1981) Excitatory amino acid transmitters. Annu Rev Pharmacol Toxicol 21:165-204.

Xu L, Rensing N, Yang XF, Zhang HX, Thio LL, Rothman SM, Weisenfeld AE, Wong M, Yamada KA (2008) Leptin inhibits 4-aminopyridine- and pentylenetetrazole-induced seizures and AMPAR-mediated synaptic transmission in rodents. J Clin Invest 118:272-280.

Yager J, Richards S, Hekmat-Scafe DS, Hurd DD, Sundaresan V, Caprette DR, Saxton WM, Carlson JR, Stern M (2001) Control of Drosophila perineurial glial growth by interacting neurotransmitter-mediated signaling pathways. Proc Natl Acad Sci U S A 98:10445-10450.

Yano S, Tokumitsu H, Soderling TR (1998) Calcium promotes cell survival through CaM-K kinase activation of the protein-kinase-B pathway. Nature 396:584-587.

Chapter 7: Appendices

During the course of my work on my thesis project itself, numerous other side projects and alternate routes of experimentation were undertaken. These alternate paths led to the collection of several data, which while not directly important to the thesis itself, should nonetheless be documented. In many cases these data represent exploratory and consequently non-hypothesis driven data collection. Often these data are from a relatively low sample size, and in some cases are even from a single sample, and thus it is difficult to subject the data to stringent critical analyses. Regardless, for the sake of posterity, I have decided to include these data here in hopes that they can be utilized by researchers in the future.
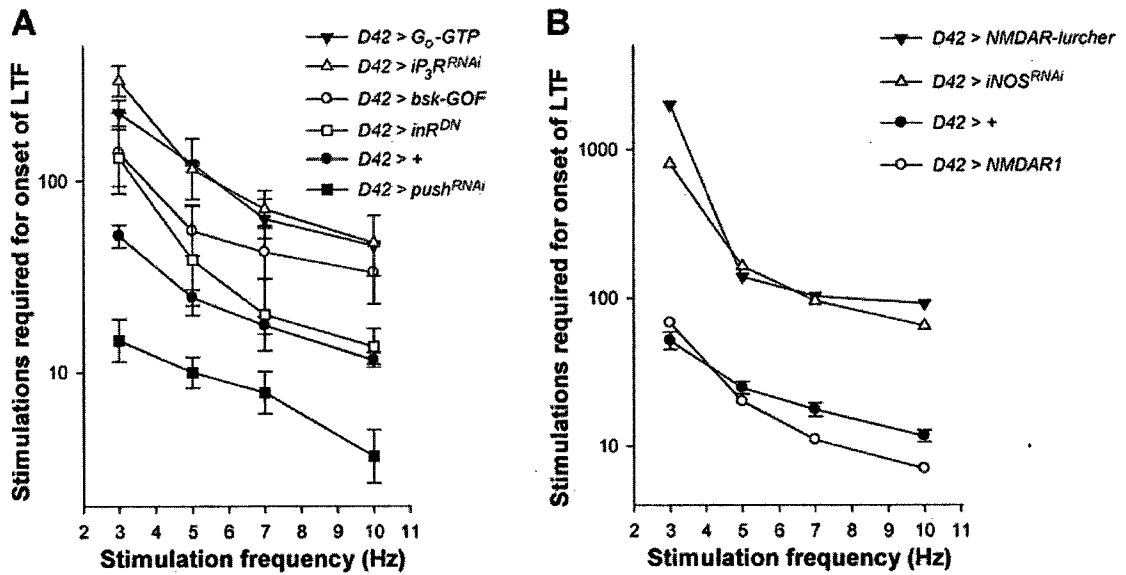
Figure 7.1. Preliminary data of transgenes expressed in motor neurons. Quantification of the rate of onset of long term facilitation for each genotype. The bath $[Ca^{2+}]$ was 0.15 mM. A 100 µM concentration of quinidine was present in the recording solution. The geometric mean of number of stimulations required for the onset of long-term facilitation at the indicated stimulus frequencies is shown for each genotype. Error bars represent SEMs. From top to bottom, n=2, 2, 5, 2, 18, and 3 respectively, for each genotype. B, Quantification of the rate of onset of long term facilitation for each genotype. The bath $[Ca^{2+}]$ was 0.15 mM. A 100 µM concentration of quinidine was present in the recording solution. The geometric mean of number of stimulations required for the onset of long-term facilitation at the indicated stimulus frequencies is shown for each genotype. Error bars represent SEMs. From top to bottom, n=1, 1, 18, and 1 respectively, for each genotype.
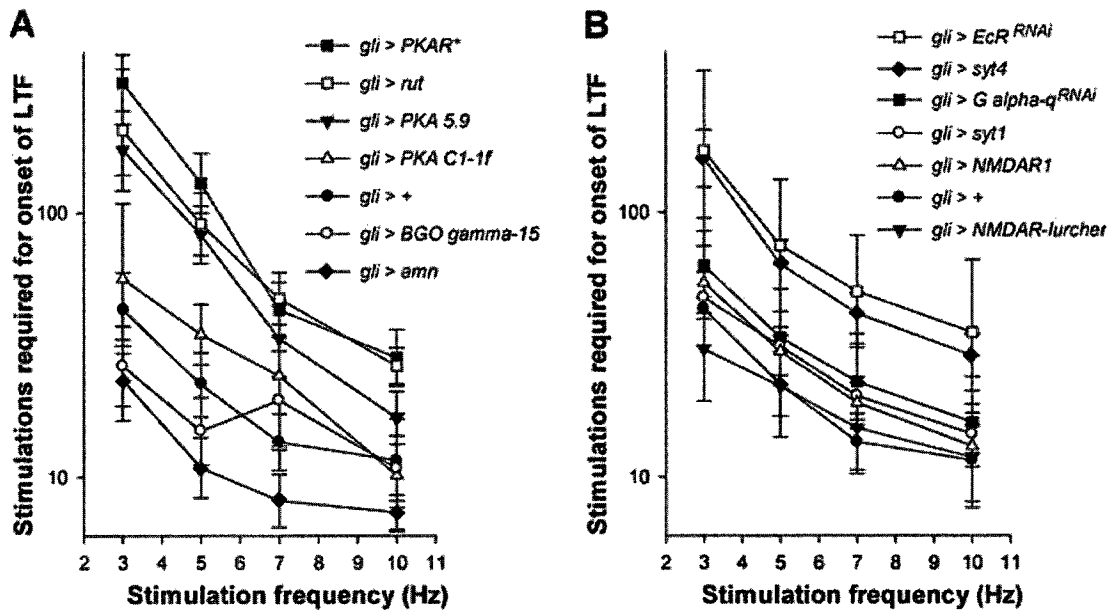
97

Figure 7.2. Preliminary data of transgenes expressed in peripheral glia. A, Quantification of the rate of onset of long term facilitation for each genotype. The bath $[Ca^{2+}]$ was 0.15 mM. A 100 µM concentration of quinidine was present in the recording solution. The geometric mean of number of stimulations required for the onset of long-term facilitation at the indicated stimulus frequencies is shown for each genotype. Error bars represent SEMs. From top to bottom, n=8, 6, 3, 4, 4, 5, and 14 respectively, for each genotype. B, Quantification of the rate of onset of long term facilitation for each genotype. The bath $[Ca^{2+}]$ was 0.15 mM. A 100 µM concentration of quinidine was present in the recording solution. The geometric mean of number of stimulations required for the onset of long-term facilitation at the indicated stimulus frequencies is shown for each genotype. Error bars represent SEMs. From top to bottom, n=5, 7, 8, 6, 5, 4, and 7 respectively, for each genotype.

98